

American Journal of Science

MAY 2016

MULTIPROXY PALEOALTIMETRY OF THE LATE OLIGOCENE-PLIOCENE OIYUG BASIN, SOUTHERN TIBET

BRIAN S. CURRIE*[†], PRATIGYA J. POLISSAR**, DAVID B. ROWLEY***, MIQUELA INGALLS***, SHANYING LI*, GERARD OLACK***, and KATHERINE H. FREEMAN[§]

ABSTRACT. The stable isotope compositions of carbonate and organic samples from the Oiyug basin in southern Tibet allows for model calculations of the Oligocene to Pliocene paleoelevation of the south central Tibetan Plateau. We measured the oxygen isotope composition of pedogenic and lacustrine calcite, dolomite, and siderite, and the hydrogen isotope composition of *n*-alkanes from plant waxes to reconstruct the $\delta^{18}\text{O}$ and δD values of Oiyug basin paleometeoric water. Calculated water isotope values from Oiyug basin carbonate and organic samples, respectively, are in close agreement, suggesting the preservation of an unaltered paleometeoric water isotopic signal in these archives.

Late Oligocene-middle Miocene paleoelevation estimates from groundwater/pedogenic calcite and lacustrine dolomite indicate basin elevations of 4.1 km +1.2/−1.6 km. Plant-wax *n*-alkanes δD and lacustrine-siderite $\delta^{18}\text{O}$ compositions of middle Miocene (~15 Ma) samples indicate paleoelevations of 5.1 km +1.3/−1.9 km. This estimated elevation is similar to the 5.4 km paleoelevation estimate based on fossil-floral physiognomy from the same stratigraphic interval. Calculated late Miocene-Pliocene paleoelevation estimates derived from the $\delta^{18}\text{O}$ composition of lacustrine marls and carbonate/siderite concretions, as well as the δD from plant wax *n*-alkanes indicate a mean elevation of 5.5 km +1.4/−2.0 km at ~5 Ma. Although calculated mean paleoelevations for the Oiyug basin all fall within the errors associated with the model calculations, the close agreement of the different paleoelevation proxies provides an additional degree of confidence in the fidelity of the calculated paleoelevations. Calculated paleoelevations indicate a possible increase in Oiyug basin elevations of ~1.4 km between the early and late Miocene. Given the modern Oiyug basin elevation of ~4.3 km, study results allow for a possible >1 km decrease in elevation since the early Pliocene. These findings, in conjunction with other Tibetan paleoaltimetry studies, are consistent with tectonic models supporting high elevations of the Tibetan Plateau since the initiation of India-Asia collision during the Eocene, and subsequent late Cenozoic extensional collapse.

Keywords: Tibetan Plateau, Oiyug Basin, paleoaltimetry, oxygen isotopes, lipid biomarkers, deuterium, Miocene

INTRODUCTION

The oxygen isotopic composition of nonmarine carbonates has been extensively used to reconstruct the isotopic composition of paleometeoric waters. Investigators have used the $\delta^{18}\text{O}$ values of paleosol and lacustrine carbonate, as well as early

* Department of Geology & Environmental Earth Science, Miami University, Oxford, Ohio 45055

** Lamont-Doherty Earth Observatory of Columbia University, 61 Route 9W, Palisades, New York 10964

*** University of Chicago, Department of Geophysical Sciences, 5734 S. Ellis Avenue, Chicago, Illinois

60637

[§] Department of Geosciences, The Pennsylvania State University, University Park, Pennsylvania 16802

[†] Corresponding author: curriebs@miamiOH.edu

digenetic cements from fluvial deposits to reconstruct paleoclimates, paleoatmospheric circulation patterns, ancient hydrological regimes, and most recently, the paleoaltimetric history of orogenic belts. In regard to stable isotope based paleoaltimetry, numerous investigations have documented the paleoelevation history of the Tibetan Plateau over the past ~55 million years (Garziona and others, 2000; Rowley and others, 2001; Currie and others, 2005; Rowley and Currie, 2006; DeCelles and others, 2007; Quade and others, 2007; Saylor and others, 2009; Ding and others, 2014; Huntington and others, 2015). These studies have relied solely on the stable isotopic composition of pedogenic and lacustrine carbonate to estimate Tibetan paleoelevations. Primary carbonate isotopic compositions, however, have the potential to be altered by burial diagenesis (Mora and others, 1998). While methods such as careful petrographic inspection, carbonate mineral characterization, and the $\delta^{18}\text{O}$ values of marine carbonate clasts in intercalated conglomerates can be used to determine if samples have been altered (DeCelles and others, 2007; Saylor and others 2009), micron-scale recrystallization may go unnoticed in sample preparation (Garziona and others, 2004; Leier and others, 2009), and lead to erroneous isotopic reconstructions of paleometeoric waters.

The use of multiple-proxy records of meteoric water isotopic composition is one mechanism to test the fidelity of isotope-based paleoelevation records. The evaluation of both the $\delta^{18}\text{O}$ values of nonmarine carbonates and δD values of early-diagenetic smectite from volcanic ash deposits have both been used to determine the oxygen and hydrogen isotopic composition of Cenozoic meteoric waters of western North America and reconstruct the elevation history of the Sierra Nevada and the Basin and Range province (Poage and Chamberlain, 2001; Horton and others, 2004). In addition, Hren and others (2010) used the δD composition of plant wax *n*-alkanes and paleotemperature estimates from microbially produced tetraethers preserved in leaf-bearing deposits to calculate >2 km Eocene paleoelevations for the Sierra Nevada. The results of this work were similar to previous paleoelevation estimates for the same region derived from the δD composition of kaolinite (Mulch and others, 2006) and volcanic glass (Cassel and others, 2009). In Tibet, Polissar and others (2009) used the δD composition of epicuticular plant wax *n*-alkanes preserved in lacustrine shales to evaluate the Eocene-Miocene paleoaltimetry of the central and northern Tibetan Plateau. Paleoelevations calculated for the Eocene–Miocene Lunpola Basin from *n*-Alkane δD values by Polissar and others (2009) were nearly identical to carbonate $\delta^{18}\text{O}$ -inferred elevations determined by Rowley and Currie (2006) from the same strata. The close correspondence of these two isotopic systems despite different archive materials, modes of incorporation, and diagenetic processes demonstrates not only the validity of stable isotope-based paleoaltimetry, but also the utility of employing multiple-proxy records.

Below we present both oxygen and hydrogen stable isotope data from Late Oligocene-Pliocene deposits of the Oiyug (Wuyu) basin in south-central Tibet to reconstruct the late Paleogene and Neogene paleoaltimetry of the southern Tibetan Plateau. Middle Miocene deposits of the Oiyug basin contain lacustrine, pedogenic, and early diagenetic carbonates that have previously been utilized to determine the $\delta^{18}\text{O}$ values of paleoprecipitation and reconstruct paleoelevations for the region (Currie and others, 2005). Our present investigation contributes additional calcite and dolomite $\delta^{18}\text{O}$ data for Oligocene, Miocene, and Pliocene strata of the basin, as well as new siderite $\delta^{18}\text{O}$ and plant-wax *n*-alkane δD values of middle Miocene-Pliocene deposits. In addition, we compare our results with revised floral physiognomic estimates of paleoelevation (Khan and others, 2014) derived from the same middle Miocene stratigraphic interval.

Our study results extend the stable-isotope record of paleoprecipitation and paleoelevation of the Oiyug Basin from late Oligocene time (<31 m.y.) into the early

Pliocene (~5 Ma). Our results also allow us to compare and contrast the calculated paleoelevations of four different paleoaltimeters as a test of the fidelity of both stable isotope- and floral physiognomy-based estimates of paleoelevation.

GEOLOGIC SETTING

The Oiyug Basin is located in south-central Tibet, ~160 km west of Lhasa. The basin is situated on the Lhasa terrane, ~60 km north of the Yarlung-Zangpo Suture and covers an area of ~300 km² (Wang and Chen, 1999) (fig. 1). The modern elevation of the basin floor ranges from ~4300 to 4400 m with surrounding areas exceeding 5600 m; the corresponding hypsometric mean of the basin region is ~5000 m. Oligocene-middle Miocene deposits of the basin are developed above an unconformity overlying Cretaceous-Paleogene intrusive and volcanic rocks (Zhu and others, 2006). During the Neogene, deposition was coeval with both volcanism and contractional deformation along the northwest flank of the basin (Zhu and others, 2006). The basin experienced a period of extensive volcanism between ~15 and 8 Ma, when as much as 1900 m of rhyo-dacitic ashflow tuffs and associated pyroclastic material were deposited (Zhu and others, 2006; Chen and others, 2008). Late Miocene-Pliocene strata in the basin are essentially flat lying and consist of an ~1 km thick assemblage of fluvial and lacustrine deposits (Zhu and others, 2006). These deposits stratigraphically on-lap older Neogene structures along the northwestern margin of the basin (fig. 1). The Miocene and younger history of the Oiyug basin occurred within an extensional setting, comparable with other regions in southern Tibet (Harrison and others, 1995; Hurtado and others, 2001; Saylor and others, 2010).

STRATIGRAPHY AND AGE

Late Paleogene-Neogene age rocks of the Oiyug basin consist of the Oligocene-lower Miocene Rigongla Formation, middle-upper Miocene Gazhacun and Zongdang Groups, and upper Miocene-Pliocene Oiyug Formation (fig. 2). Partial stratigraphic sections of the Rigongla Formation (fig. 3) and Gazhacun Group (fig. 4) were measured along the Ramaqu and Badamaqen drainages in the northern part of the Oiyug Basin (fig. 1). A partial section of the lower-middle part of the Oiyug Formation (fig. 5) was measured in the southwestern part of the basin (fig. 1).

The Oligocene-Miocene Rigongla Formation consists of dacitic to andesitic volcanics, interbedded within an overall upward-fining, >500 meter-thick sequence of conglomerates, sandstones, and mudstones. Dacites in the lower Rigongla Formation yielded a K-Ar age of 31.4 Ma (Zhu and others, 2006), providing a maximum age of deposition for the unit. Above the volcanics, the upper Rigongla Formation consists of ~150 to 200 m of alluvial fan and fluvial-channel conglomerates, sandstones and intercalated fluvial-overbank lithologies (fig. 3). Overbank deposits in the interval contain crevasse splay sandstones and floodplain siltstones, mudstones, and shales. Some mudstones in the Rigongla Formation contain groundwater carbonate horizons consisting of micritic nodules (3–15 cm in diameter) developed in beds displaying limited pedogenic modification. These nodules were sampled for isotopic analysis.

The Gazhacun Group consists of up to ~450 m of mudstone, shale, coal, sandstone, and conglomerate, and volcanoclastic deposits (fig. 4). The Gazhacun Group described here was classified as the Manxiang Formation by Zhu and others (2006). The lower part of the Gazhacun Group rests directly on volcanics of the Rigongla Formation and consists of ~140 m of red and gray overbank mudstone and occasional lenticular fluvial channel sandstones and conglomerates. Overbank mudstones contain paleosol horizons containing root traces, translocated clay accumulations, subangular/angular blocky peds, slickensided-ped surfaces, and well-developed pedogenic calcite nodules ranging from between 0.25 and 1.5 cm in diameter. Paleosol carbonate nodules for isotopic analysis were sampled from clay-rich

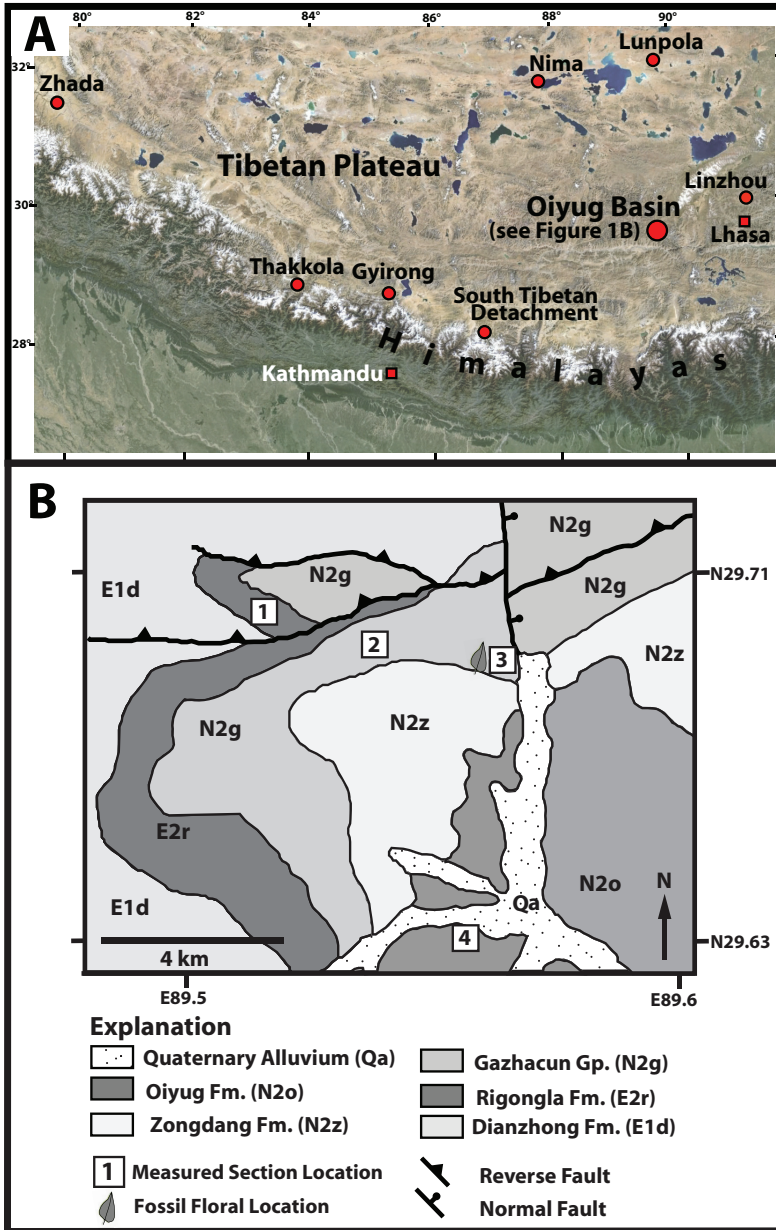


Fig. 1. (A) Landsat image of south-central Tibetan Plateau and Himalaya showing the location of the Oiyug basin and other paleoaltimetry localities discussed in the text. (B) Geologic map of Oiyug basin showing measured section locations and location of fossil floral locality of Spicer and others (2003) and Khan and others (2014). Map modified from Zhou and others (2010a).

(Btk) horizons 50 to 80 cm below the interpreted tops of soils. Groundwater carbonate nodules similar to those in the Rigongla Formation were also sampled.

The middle part of the Gazhacun Group consists of ~225 m of gray, green, and light red shale and mudstone, and thin to very-thin beds of siltstone and fine-grained

Age (Ma)	Age	Unit	Lithologies	Radiometric/ Paleomagnetic age (Ma)
5	Pliocene	Oiyug Fm.	lacustrine shale/mudstone, marl, nodular siderite/calcite	2.5
10	Miocene	Zongdang Gp.	tuffaceous sandstone/conglomerate dacitic/andesitic/rhyolitic volcanics	8.1
				7.92±0.15 8.23±0.13 9.87±0.30
15	Miocene	Gazhacun Gp.	Upper: lacustrine shale, sandstone, siderite, coal, felsic tuff	15.03±0.11
20			Middle: lacustrine shale/mudstone, marl, nodular dolomite/ siderite	15.10±0.49
25	Oligocene	Rigongla Fm.	Lower: fluvial sandstone, overbank mudstone, groundwater/ pedogenic carbonate	
30			alluvial fan/fluvial conglomerate, sandstone; overbank mudstone, groundwater carbonate nodules	
			dacitic volcanics	31.4

Fig. 2. Time-stratigraphic chart and generalized lithological descriptions for Oligocene-Pliocene strata of the Oiyug basin. Compiled from Spicer and others (2003), Zhu and others (2006), Chen and others (2008), and Zhou and others (2010a).

sandstone that were deposited in lacustrine and lacustrine-marginal environments. The middle Gazhacun also contains lenticular fluvial channel sandstones, and red overbank mudstones containing pedogenic carbonate nodules. Fine-grained lacustrine intervals contain microcrystalline, early-diagenetic dolomite nodules as evidenced by the differential compaction of surrounding mudstone lithologies (Currie and others, 2005). Samples for isotopic analysis from the middle Gazhacun Group include dolomite nodules derived from lacustrine/lacustrine-margin deposits, as well as pedogenic carbonate nodules from overbank mudstones.

The upper part of the Gazhacun Group consists of ~100 m of tuffaceous conglomerate and sandstone with interbeds of carbonaceous siltstone, mudstone, shale, and coal interbedded with ashflow tuffs. Deposition in the interval is interpreted to have occurred in fluvial channel, floodplain, lacustrine, and swamp environments (Spicer and others, 2003; Zhu and others, 2006). Several tuffaceous siltstone and fine-grained sandstone beds in the upper part of the unit contain well-preserved leaf fossils (Spicer and others, 2003). The upper Gazhacun Group also contains several 1 to 3 m thick beds of ash flow tuff with abundant biotite and feldspar crystals. Sanidine sampled from a reworked tuff in the middle part of the formation yielded a ^{40}Ar - ^{39}Ar age of 15.10 ± 0.49 Ma (Spicer and others, 2003). The age of the top of the unit is constrained by the 15.03 ± 0.11 Ma age of the conformably overlying Zongdang Group (Spicer and others, 2003; see below). Early diagenetic siderite nodules and carbonaceous mudstone/shale from the upper part of the Gazhacun Group were sampled for isotopic analysis.

The middle to late Miocene Zongdang Group consists of up to ~1900 m of dacite, andesite, trachyte, and trachyandesite, ash flow-tuffs, and volcanoclastic deposits (Zhu

Ramaqu Headwaters Section Upper Rigongla Formation

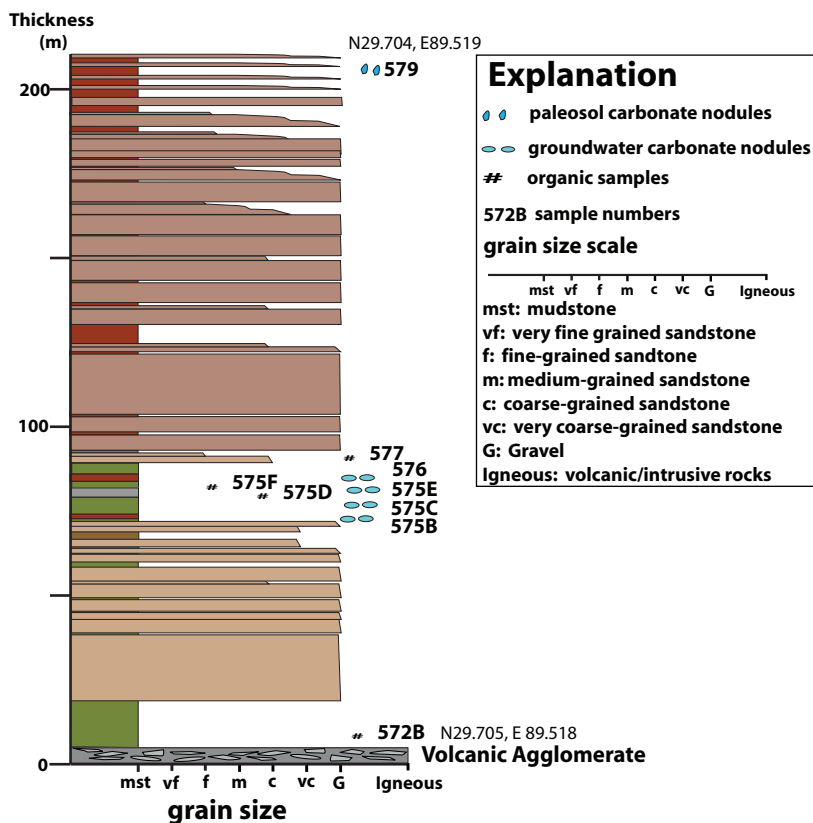


Fig. 3. Partial stratigraphic section log of the upper Rigongla Formation in the headwaters of the Ramachu, northwestern Oiyug basin. See figure 1 for location. Latitude/longitude for the base and top of the section are shown in figure. Section colors in electronic version approximate lithologic colors observed in the field.

and others, 2006; Chen and others, 2008). Rocks of the Zongdang Group described here have been previously classified as the Laiqing Formation by Zhu and others (2006). The lower portion of the Zongdang Group is dominated by lava flows and cross-cutting dikes, while the upper parts of the unit consists primarily of ash-flow tuffs and volcanoclastic sandstones and conglomerates (Zhu and others, 2006).

A dacite sampled from the lower Zongdang Group in the eastern part of the Oiyug basin yielded an ^{40}Ar - ^{39}Ar age of 15.48 ± 0.11 (Zhou and others, 2010a), indicating that the unit, in part is laterally correlative to the underlying Gazhacun Group. Dacites, trachytes and trachyandesites sampled from the lower parts of the Zongdang Group along the north flank of basin yielded ^{40}Ar - ^{39}Ar ages ranging from 15.03 ± 0.11 Ma to 12.57 ± 0.08 (Spicer and others, 2003; Zhou and others, 2010a). An andesite from the top of the lower Zongdang along the southwestern flank of the basin was dated by K-Ar to 9.87 ± 0.30 Ma, while ash flow tuffs from the upper-most Zongdang Group yielded K-Ar dates ranging from 8.23 ± 0.13 Ma to 7.92 ± 0.15 Ma (Chen and others, 2008).

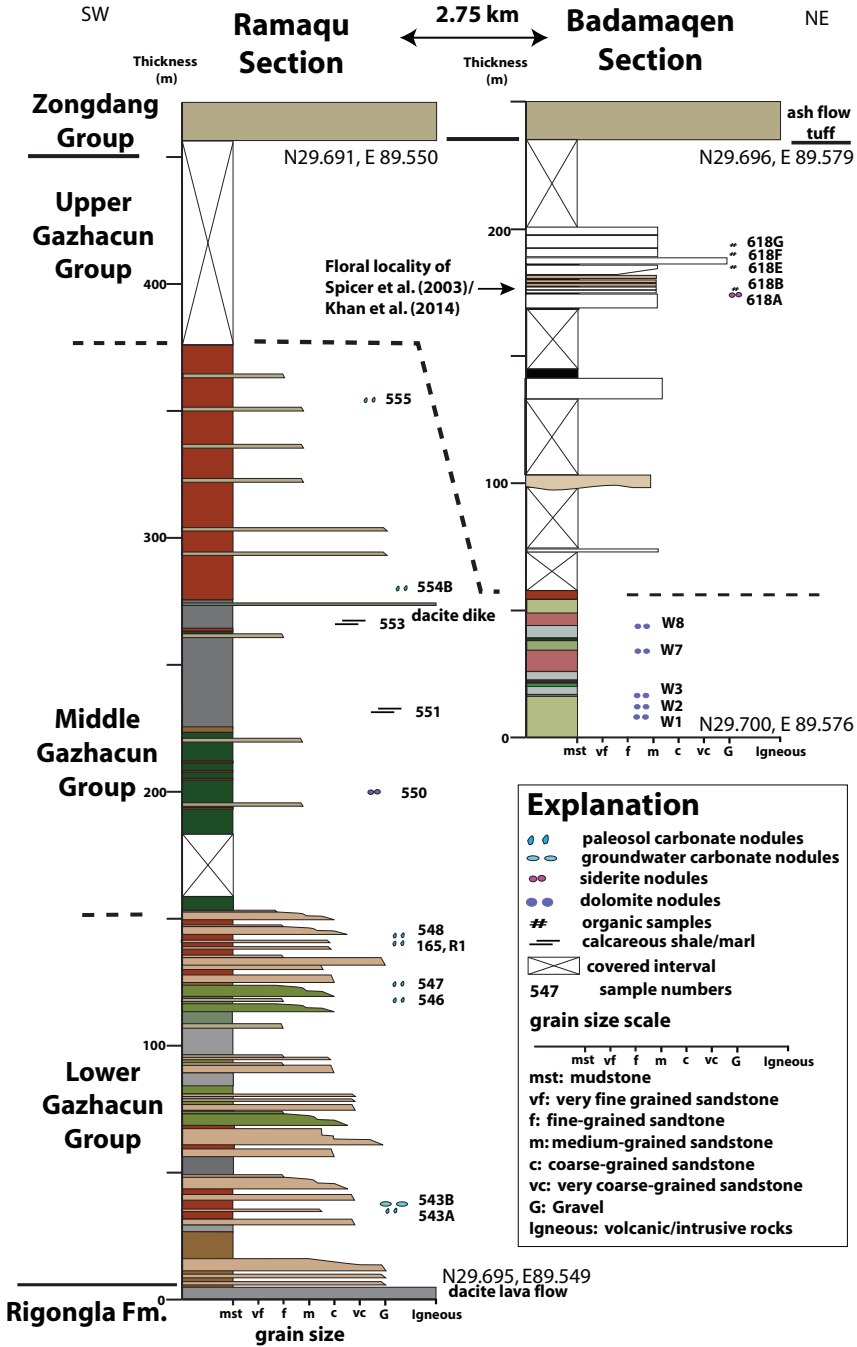


Fig. 4. Stratigraphic section log of the Gazhacun Group along the Ramachu and Badamaqen drainages, northwestern Oiyug basin. See figure 1 for location. Latitude/longitude for the base and top of each section are shown in figure. Section colors in electronic version approximate lithologic colors observed in the field.

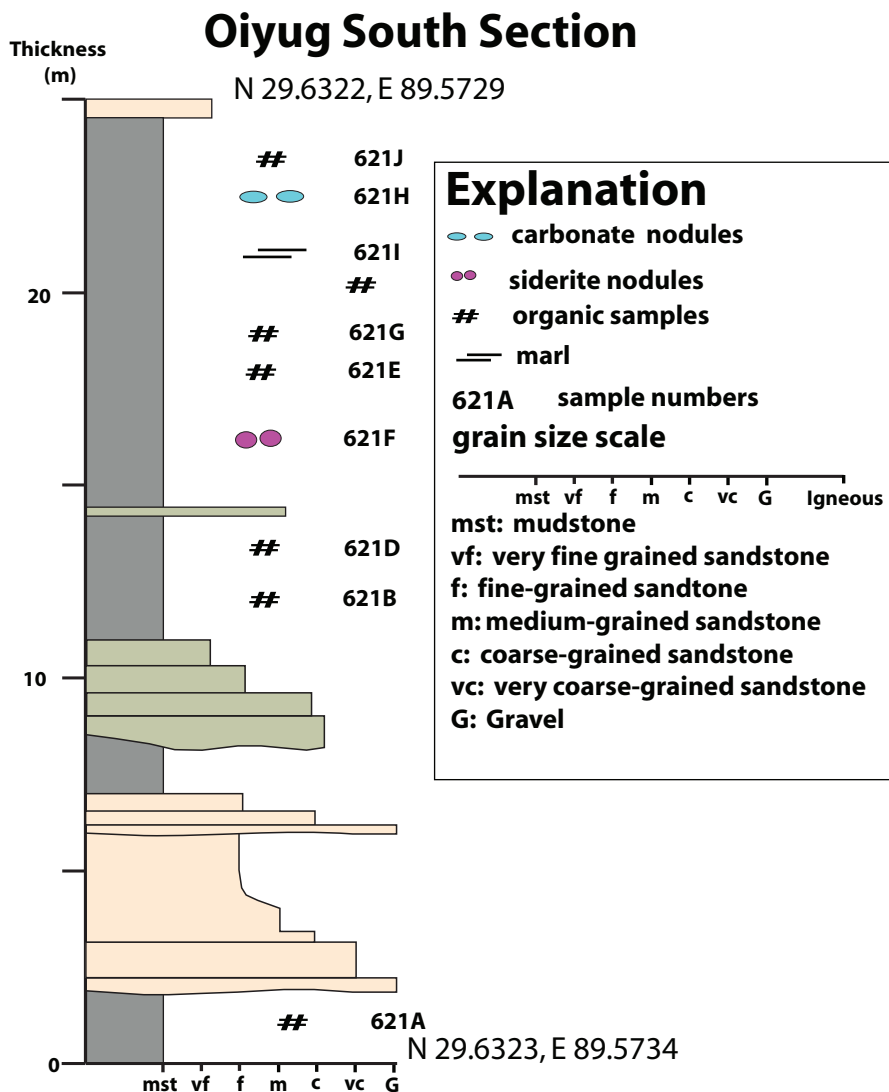


Fig. 5. Partial stratigraphic section log of the Oiyug Formation, western Oiyug basin. See figure 1 for location. Latitude/longitude for the base and top of the section are shown in figure. Section colors in electronic version approximate lithologic colors observed in the field.

The upper Miocene-Pliocene Oiyug Formation overlies the Zongdang Group. The Oiyug Formation consists of >1000 m of volcanoclastic sandstone and conglomerate, and mudstone, shale, marl, and lignite (Zhu and others, 2006). Deposition is interpreted to have occurred in a basin-centered lacustrine system with associated fan delta, fluvial, overbank and swamp deposition occurring along the basin margins (Zhu and others, 2006).

In the central part of the basin, the Oiyug Formation is interpreted as being conformable with the underlying upper Zongdang Group (Zhu and others, 2006). Along the basin margins however, the Oiyug Formation stratigraphically onlaps

deformed strata of underlying middle-upper Miocene units (Zhu and others, 2006; Chen and others, 2008).

A late Miocene-Pliocene depositional age (~ 8.1 – 2.5 Ma) for the Oiyug Formation is indicated from a magnetostratigraphic study of the unit conducted in the southeastern part of the basin (Chen and others, 2008). Lacustrine marl, calcium carbonate nodules, and organic-rich shale/mudstone sampled as part of this investigation were derived from the middle part of the Oiyug Formation (fig. 5) and have an interpreted depositional age of ~ 5 Ma (Chen and others, 2008).

STABLE-ISOTOPE GEOCHEMISTRY

In order to determine the oxygen isotopic composition of Paleogene-Neogene Oiyug Basin paleometeoric waters, pedogenic calcite nodules and early-diagenetic lacustrine calcite, dolomite, and siderite nodules were collected from the Rigongla and lower Gazhacun formations. Vein calcites associated with two separate calcite nodules were also sampled. Lacustrine siderite nodules from the upper Gazhacun Formation, and lacustrine calcite nodules and marls from the Oiyug Formation were also collected. Sample petrography and the effects of potential diagenetic alteration were determined using both petrographic and scanning electron microscopy. The mineralogical composition of collected samples was further confirmed by X-ray powder diffraction. Additional details on the methodology used in carbonate sample preparation and stable-isotope analyses are outlined in Appendix A.

Estimates of the hydrogen-isotopic composition of Oiyug Basin paleoprecipitation were determined from *n*-alkanes derived from leaf waxes extracted from organic-rich mudstones and shales from the upper Gazhacun and Oiyug formations. Samples were processed and analyzed following the methods of Polissar and others (2009) and Polissar and Freeman (2010) (see Appendix A).

Carbonate Stable Isotope Results

The results of our stable isotope analyses of Oiyug Basin carbonates are listed in table 1. Pedogenic calcium carbonate nodules from the Rigongla and Gazhacun formations have $\delta^{18}\text{O}_c$ values that range from -11.49‰ to -20.05‰ (VPDB), with $\delta^{13}\text{C}$ values of -8.58‰ to -5.52‰ (table 1). Groundwater carbonates from the Rigongla and lower Gazhacun formations yielded $\delta^{18}\text{O}_c$ values that range from -13.94‰ to -19.5‰ , with $\delta^{13}\text{C}$ values ranging from -2.60‰ to -3.76‰ . Secondary vein calcite sampled from pedogenic and groundwater nodules in the lower Gazhacun Formation have $\delta^{18}\text{O}_c$ values of -25.54‰ and -27.07‰ .

The $\delta^{18}\text{O}$ values of the nodular dolomite samples from the middle part of the Gazhacun Formation range from -11.31‰ , to -5.5‰ , with $\delta^{13}\text{C}$ values of -9.5‰ to -5.1‰ . Samples of calcareous mudstone and shale interbedded with the nodular-dolomite samples have $\delta^{18}\text{O}$ compositions of -11.6‰ and -13.0‰ , respectively. The $\delta^{13}\text{C}$ values of the same samples were -3.75‰ and -2.50‰ .

An early-diagenetic siderite nodule sampled from carbonaceous mudstone of the upper Gazhacun Formation has a $\delta^{18}\text{O}$ value of -18.4‰ and $\delta^{13}\text{C}$ value of 4.12‰ . The marl and calcium carbonate nodule samples from the Oiyug Formation have extremely negative $\delta^{18}\text{O}_c$ values of -27.9‰ and -27.3‰ , respectively (table 1). A siderite nodule sampled from the Oiyug Formation yielded a $\delta^{18}\text{O}$ value of -11.45‰ and an extremely positive $\delta^{13}\text{C}$ value of 12.93‰ .

Potential diagenetic effects on original $\delta^{18}\text{O}$ values.—The use of authigenic carbonates to interpret regional paleoelevations hinges on the assumption that the measured stable-isotopic composition of lacustrine and paleosol carbonates accurately record the composition of meteoric waters at the time of deposition. Diagenetic alteration associated with high-temperature fluids or younger more negative meteoric waters can

TABLE 1
Oiyug Basin carbonate $\delta^{13}\text{C}$ and $\delta^{18}\text{O}$ values

Section	Formation	Sample	Lithology/ Mineralogy	$\delta^{13}\text{C}$ (vpdb)	$\delta^{18}\text{O}$ (vpdb)	$\delta^{18}\text{O}$ (vsmow)	Lab+
Oiyug NW	Oiyug	621H	nod calcite	-0.77	-27.40	2.61	A
Oiyug NW	Oiyug	621I	marl calcite	1.32	-28.00	1.99	A
Oiyug NW	Oiyug	621F	nod siderite	12.93	-11.45	19.05	C
Badamaqen	U. Gazhacun	618A	nod siderite	4.12	-18.40	11.87	C
Lower Ramaqu	M. Gazhacun	555	ped calcite	-5.52	-19.97	10.27	A
Lower Ramaqu	M. Gazhacun	554B	ped calcite	-8.58	-11.49	19.02	C
Badamaqen	M. Gazhacun	W8*	nod dolomite	-7.30	-7.60	23.03	A
Badamaqen	M. Gazhacun	W7*	nod dolomite	-5.40	-5.50	25.19	A
Badamaqen	M. Gazhacun	W3*	nod dolomite	-6.30	-5.70	24.98	A
Badamaqen	M. Gazhacun	W2*	nod dolomite	-5.10	-5.50	25.19	A
Badamaqen	M. Gazhacun	W1*	nod dolomite	-5.40	-5.80	24.88	A
Lower Ramaqu	M. Gazhacun	553	calc shale	-3.75	-13.00	17.46	C
Lower Ramaqu	M. Gazhacun	551	calc shale	-2.50	-11.64	18.86	C
Lower Ramaqu	M. Gazhacun	550	nod dolomite	-9.50	-11.31	19.21	A
Lower Ramaqu	L. Gazhacun	548	ped calcite	-7.63	-20.07	10.17	A
Lower Ramaqu	L. Gazhacun	165Ca*	ped calcite	-6.90	-19.80	10.45	A
Lower Ramaqu	L. Gazhacun	165D*	ped calcite	-7.10	-20.00	10.24	A
Lower Ramaqu	L. Gazhacun	165Fa*	ped calcite	-6.90	-19.70	10.55	A
Lower Ramaqu	L. Gazhacun	165Fb*	ped calcite	-6.80	-19.70	10.55	A
Lower Ramaqu	L. Gazhacun	165Fc*	ped calcite	-5.90	-18.00	12.30	A
Lower Ramaqu	L. Gazhacun	165G*	ped calcite	-6.80	-19.60	10.66	A
Lower Ramaqu	L. Gazhacun	R2*	ped calcite	-7.00	-20.20	10.04	A
Lower Ramaqu	L. Gazhacun	547	ped calcite	-5.99	-19.07	11.20	H
Lower Ramaqu	L. Gazhacun	546	ped calcite	-7.23	-21.05	9.16	C
Lower Ramaqu	L. Gazhacun	543B	gw calcite	-3.31	-19.53	10.73	C
Lower Ramaqu	L. Gazhacun	543AV	vein calcite	-2.95	-27.07	2.95	H
Lower Ramaqu	L. Gazhacun	543A	ped calcite	-7.64	-19.43	10.83	H
Upper Ramaqu	U. Rigongla	579	ped calcite	-6.75	-18.91	11.36	A
Upper Ramaqu	U. Rigongla	576V	vein calcite	-3.81	-25.54	4.54	A
Upper Ramaqu	U. Rigongla	576	gw calcite	-3.37	-20.40	9.83	A
Upper Ramaqu	U. Rigongla	575E	gw calcite	-3.72	-11.86	18.63	A
Upper Ramaqu	U. Rigongla	575C	gw calcite	-2.60	-16.82	13.52	A
Upper Ramaqu	U. Rigongla	575B	gw calcite	-3.76	-13.94	16.49	A

* Sample included in Currie and others (2005).

Denotes laboratory that conducted analysis: A:University of Arizona; C:University of Chicago; H:Harvard University.

decrease $\delta^{18}\text{O}$ values and lead to erroneous paleoelevation interpretations (Garziona and others, 2004).

Several lines of evidence lead us to conclude that overall diagenetic alteration of our samples has been minimal. First, all samples were derived from micritic carbonates that display little evidence of recrystallization. While the effects of diagenesis on carbonates can be subtle (Leier and others, 2009), our samples do not display pervasive microcrystallization that is suggestive of isotopic re-equilibration (Garziona and others, 2004). In addition, observed variability in isotopic composition within our sample suite does not display any vertical stratigraphic trends (for example systematically decreasing $\delta^{18}\text{O}$ values with depth) that could be attributed to burial diagenesis.

Investigations on the potential of burial diagenesis to alter the original $\delta^{18}\text{O}$ composition of pedogenic carbonates indicates no significant alteration at burial temperatures

of $< 100^{\circ}$ to 125°C (Mora and others, 1998; Quade and others, 2013). Thermal Alteration Index values determined from pollen and spores from mudstone/shale samples from our Oiyug Basin measured sections correspond to vitrinite reflectance values (R_0) of 0.3 percent to 0.8 percent, indicating burial temperatures ranging from 23°C to 125°C , respectively (table B1) (Barker 1998). Thermal maturity determinations from molecular biomarkers of the Oiyug and upper Gazhacun units (see below) also point towards relatively modest burial temperatures. The highest burial temperatures (95 – 125°C), observed in the lower and middle part of the Rigongla Formation, are at the lower boundary where isotopic resetting may have occurred. Vein calcite cross cutting pedogenic and groundwater carbonate nodules in this interval are approximately 5% to 7.5% more negative than their host samples, and indicates the veins likely precipitated at higher temperatures (and/or from more negative meteoric waters) than the original carbonate. In addition, the carbonate samples throughout this stratigraphic interval are dense micritic pedogenic and groundwater carbonates that developed in, and are intercalated with, clay-rich lithologies. This association suggests that any diagenetic recrystallization that may have occurred under rock-buffered, fluid-poor conditions that would have led to a minimal alteration of original isotopic compositions (Bera and others, 2010; Quade and others, 2013).

An evaluation of the isotopic compositions of Gazhacun Group and Oiyug Formation siderite samples provide an additional test of potential diagenetic alteration. Siderites provide a more robust measurement of $\delta^{18}\text{O}$ because, unlike other carbonate minerals, they do not readily undergo isotopic exchange during burial diagenesis due to higher equilibration temperatures (Curtis and others, 1975; Rezaee and others, 1997). The $\delta^{18}\text{O}$ values of the siderite samples in the study (-17.1% , -10.8%) are within the range of $\delta^{18}\text{O}$ values from dolomite and calcite samples. In addition, calculated meteoric water compositions ($\delta^{18}\text{O}_w$) derived from these sample values also falls within the range of those from Oiyug Basin calcite samples (see below), suggesting all of our samples have experienced minimal diagenetic alteration.

Calculated meteoric water $\delta^{18}\text{O}$ compositions.—The $\delta^{18}\text{O}$ values of authigenic carbonate such as those sampled from the Oiyug Basin have been used extensively as a proxy for the composition of meteoric water (McKenzie, 1982; Kelts and Talbot, 1989; among others). Because of the temperature dependence of carbonate-water fractionation, in order to determine the isotopic composition of the water from which ancient carbonates precipitated, it is necessary to have an estimated paleotemperature. Absent direct carbonate Δ_{47} precipitation temperatures (for example Ghosh and others, 2006), other paleotemperature proxies must be employed. In this regard, we rely on demonstrated relationships between temperature and the precipitation of the different carbonate types contained in our Oiyug Basin sample suite.

As the majority of both pedogenic and lacustrine carbonates are thought to form during the warmest months of the year (Talbot, 1990; Drummond and others, 1995; Rosen and others, 1995; Teranes and others, 1999; Quade and others, 2013), estimates of warm month mean temperature (WMMT) are most useful. Recent fossil leaf physiognomic studies from Gazhacun Formation in the Oiyug Basin indicate Mean Annual Temperature of $8.2 \pm 2.8^{\circ}\text{C}$, and a WMMT value of $\sim 23.8 \pm 3.4^{\circ}\text{C}$ (Kahn and others, 2014). Recent work on the Δ_{47} precipitation temperature of pedogenic carbonate indicates they commonly form in the subsurface at temperatures up to 15°C higher than the regional MAT (Quade and others, 2013). Given the estimated $\sim 8^{\circ}\text{C}$ MAT for the middle Miocene Oiyug Basin, the floral-derived WMMT of $23.8 \pm 3.4^{\circ}\text{C}$ would fall at the upper range of expected precipitation temperatures for our pedogenic carbonate samples. Therefore we use the WMMT as a best estimate for the precipitation temperature of the pedogenic carbonates and the error derived from the WMMT range (19.6°C – 26.4°C) determined by Khan and others (2014) to calculate

the uncertainty in isotopic compositions of the meteoric waters from which sampled Oiyug pedogenic carbonates precipitated (table 2).

In order to constrain the possible precipitation temperatures for the lacustrine carbonates sampled in this study, we employ the $\sim 15^\circ$ to 30°C range of temperature at which most modern lacustrine micritic carbonates precipitate (Talbot, 1990; Drummond and others, 1995; Rosen and others, 1995; Teranes and others, 1999; Hren and Sheldon, 2012). For the groundwater carbonates sampled from the Oiyug Basin, studies on modern shallow groundwater temperatures indicate that average temperatures are $\sim 2^\circ\text{C}$ greater than local mean annual temperature, but can demonstrate seasonal fluctuations of $\pm 10^\circ$ (Heath, 1983). Given this relationship and the floral-derived mid-Miocene Oiyug Basin MAT of $8.2 \pm 2.8^\circ\text{C}$ determined by Khan and others (2014), Oiyug groundwater carbonates would have precipitated between $\sim 0.2^\circ$ and 20.2°C . We employ this broad range of temperatures when calculating potential meteoric water compositions from Oiyug groundwater carbonates. Given likely similarities between groundwater temperatures and shallowly buried lacustrine deposits, this same temperature range is used to calculate the isotopic composition of the meteoric waters from which Oiyug Basin lacustrine calcite, dolomite, and siderite nodules precipitated (table 2).

Using the above temperature ranges, the fractionation factors for calcite-water (Kim and O'Neil, 1997), dolomite-water (Vasconcelos and others, 2005), and siderite-water (Zhang and others, 2001), and assuming equilibrium, Oiyug Basin carbonates sampled for this study precipitated from meteoric waters with mean $\delta^{18}\text{O}_w$ values ranging from $-28.24 \pm 2.52\text{‰}$ (± 2 standard error of the mean, s.e.m.) to $-8.52 \pm 0.77\text{‰}$ (VSMOW) (table 2). The wide range of values for these samples was likely governed by the ancient hydrology of the Oiyug Basin. For example, there is a systematic variation in $\delta^{18}\text{O}_w$ values that correspond to different carbonate types. With the exception of one sample, pedogenic calcite nodules display a tight cluster of $\delta^{18}\text{O}_c$ values ranging from -18.00‰ to -21.05‰ (VPDB) (fig. 6). Corresponding mean $\delta^{18}\text{O}_w$ values for these samples range from $-15.05 \pm 0.76\text{‰}$ to $-18.11 \pm 0.76\text{‰}$ (VSMOW). In contrast, the $\delta^{18}\text{O}_c$ composition of groundwater calcite nodules and lacustrine calcite nodules/marl ranges from -11.64‰ to -28.00‰ (VPDB), with calculated $\delta^{18}\text{O}_w$ compositions ranging from $-9.86 \pm 1.77\text{‰}$ to $-28.24 \pm 2.52\text{‰}$ (VSMOW). These differences likely reflect the higher potential for evaporative enrichment of meteoric waters in lacustrine and groundwater systems relative to soil waters, and are consistent with similar interpretations of isotopic variation documented in other depositional basins (Kelts and Talbot, 1989; Bera and others, 2010). This hypothesis is further supported by the $\delta^{18}\text{O}_d$ compositions of middle Gazhacun Group dolomite nodules, which are the most positive values in the sample suite (-5.50‰ to -11.31‰ (VPDB)). These values correspond to $\delta^{18}\text{O}_w$ values of -9.42 to $-15.19 \pm 2.74\text{‰}$ (VSMOW), and likely reflect precipitation from the most evaporation-enriched waters during middle Gazhacun Group deposition (Currie and others, 2005).

Calculated meteoric water values of the two siderite samples are $\delta^{18}\text{O}_w -21.61 \pm 2.55\text{‰}$ for the upper Gazhacun Group, and $-14.67 \pm 2.57\text{‰}$ for the Oiyug Formation. These compositions are similar to the $\delta^{18}\text{O}_w$ values calculated from other Oiyug Basin carbonates and suggests that the calcite/dolomite samples have not been significantly affected by diagenetic alteration.

Lipid Geochemistry Results

Thermal maturity and source.—Heating and thermal maturation of organic matter can alter the hydrogen isotopic composition of long-chain *n*-alkanes through isotopic exchange and the generation of petroleum *n*-alkanes at concentrations that overwhelm the original plant-wax *n*-alkanes. An assessment of thermal maturity was made by evaluating visual Thermal Alteration Index (TAI) values of pollen and spores preserved in the stratigraphic interval. Organic samples for this component of the

TABLE 2
Paleometeoric water $\delta^{18}O$ values and paleoelevation calculations determined from Oiyug Basin carbonate isotopic compositions

Section	Formation	Sample	Lithology	$\delta^{18}O$ (vpdb)	$\delta^{18}O$ (vsnow)	Mean $\delta^{18}O_w$ (% vsnow)	2 s.e.m. (\pm %)	$\Delta\delta^{18}O_w$ (% vsnow)	$\Delta\delta^{18}O_w$ 2 s.e.m (\pm ‰)	Model Elevation (m)	2 σ Model Uncert. (+m)	2 σ Model Uncert. (-m)
Paleosol Carbonate Nodules												
Lower Ramaqu	M. Gazhacun	555	ped calcite	-19.97	10.27	-17.03	0.76	-10.4	1.1	4111	1165	-1656
Lower Ramaqu	M. Gazhacun	554B	ped calcite	-11.49	19.02	-8.52	0.77	-1.9	1.1	1115	362	-515
Lower Ramaqu	L. Gazhacun	548	ped calcite	-20.07	10.17	-17.13	0.76	-10.5	1.1	4134	1170	-1662
Lower Ramaqu	L. Gazhacun	165Ca	ped calcite	-19.80	10.45	-16.86	0.76	-10.3	1.1	4070	1157	-1644
Lower Ramaqu	L. Gazhacun	165D	ped calcite	-20.00	10.24	-17.06	0.76	-10.5	1.1	4117	1166	-1657
Lower Ramaqu	L. Gazhacun	165Fa	ped calcite	-19.70	10.55	-16.76	0.76	-10.2	1.1	4046	1152	-1637
Lower Ramaqu	L. Gazhacun	165Fb	ped calcite	-19.70	10.55	-16.76	0.76	-10.2	1.1	4046	1152	-1637
Lower Ramaqu	L. Gazhacun	165Fc	ped calcite	-18.00	12.30	-15.05	0.77	-8.5	1.1	3611	1058	-1502
Lower Ramaqu	L. Gazhacun	165G	ped calcite	-19.60	10.66	-16.66	0.76	-10.1	1.1	4022	1147	-1630
Lower Ramaqu	L. Gazhacun	R2	ped calcite	-20.20	10.04	-17.26	0.76	-10.7	1.1	4163	1175	-1671
Lower Ramaqu	L. Gazhacun	547	ped calcite	-19.07	11.20	-16.12	0.76	-9.5	1.1	3891	1120	-1591
Lower Ramaqu	L. Gazhacun	546	ped calcite	-21.05	9.16	-18.11	0.76	-11.5	1.1	4353	1212	-1723
Lower Ramaqu	L. Gazhacun	543A	ped calcite	-19.43	10.83	-16.49	0.76	-9.9	1.1	3981	1139	-1617
Upper Ramaqu	U. Rigongla	579	ped calcite	-18.91	11.36	-15.97	0.76	-9.4	1.1	3852	1111	-1579
Section	Formation	Sample	Lithology	$\delta^{18}O$ (vpdb)	$\delta^{18}O$ (vsnow)	Mean $\delta^{18}O_w$ (% vsnow)	2 s.e.m. (\pm %)	$\Delta\delta^{18}O_w$ (% vsnow)	$\Delta\delta^{18}O_w$ 2 s.e.m (\pm ‰)	Model Elevation (m)	2 σ Model Uncert. (+m)	2 σ Model Uncert. (-m)
Lacustrine Shale/Marl												
Oiyug NW	Oiyug	621I	marl calcite	-28.00	1.99	-26.25	1.74	-21.6	1.9	6080	1460	-2104
Lower Ramaqu	M. Gazhacun	551	calc shale	-11.64	18.86	-9.86	1.77	-3.3	2.0	1770	563	-801
Lower Ramaqu	M. Gazhacun	553	calc shale	-13.00	17.46	-11.22	1.77	-4.6	2.0	2349	732	-1040

TABLE 2
(continued)

Section	Formation	Sample	Lithology	$\delta^{18}\text{O}$ (vpdb)	$\delta^{18}\text{O}$ (vsmow)	Mean $\delta^{18}\text{O}_w$ (% vsmow)	2 s.e.m. (\pm %)	$\Delta\delta^{18}\text{O}_w$ (% vsmow)	2 s.e.m. (\pm %)	$\Delta\delta^{18}\text{O}_w$ (\pm %)	Model Elevation (m)	2 σ Model Uncert. (+m)	2 σ Model Uncert. (-m)
						(c)	(d)	(e)	(f)	(g)	(h)	(i)	(j)
Groundwater Calcite Nodules													
Lower Ramaqu	L. Gazhacun	543B	gw calcite	-19.53	10.73	-20.38	2.54	-13.8	2.7	4812	1290	-1839	
Upper Ramaqu	U. Rigongla	576	gw calcite	-20.40	9.83	-21.25	2.54	-14.7	2.7	4973	1315	-1877	
Upper Ramaqu	U. Rigongla	575E	gw calcite	-11.86	18.63	-12.72	2.56	-6.1	2.7	2900	883	-1253	
Upper Ramaqu	U. Rigongla	575C	gw calcite	-16.82	13.52	-17.68	2.55	-11.1	2.7	4258	1194	-1697	
Upper Ramaqu	U. Rigongla	575B	gw calcite	-13.94	16.49	-14.79	2.56	-8.2	2.7	3539	1041	-1479	
Lacustrine Calcite Nodules													
Oiyug NW	Oiyug	621H	nod calcite	-27.40	2.61	-28.24	2.52	-23.6	2.6	6332	1486	-2143	
Lacustrine Siderite Nodules													
Oiyug NW	Oiyug	621F	nod siderite	-11.45	19.05	-14.67	2.57	-10.1	2.7	4026	1148	-1631	
Badamaqen	U. Gazhacun	618A	nod siderite	-18.40	11.87	-21.61	2.55	-15.0	2.6	5038	1325	-1892	
Lacustrine Dolomite Nodules													
Badamaqen	M. Gazhacun	W8	nod dolomite	-7.60	23.03	-11.51	2.75	-4.9	2.9	2463	764	-1086	
Badamaqen	M. Gazhacun	W7	nod dolomite	-5.50	25.19	-9.42	2.75	-2.8	2.9	1567	502	-714	
Badamaqen	M. Gazhacun	W3	nod dolomite	-5.70	24.98	-9.62	2.75	-3.0	2.9	1661	530	-754	
Badamaqen	M. Gazhacun	W2	nod dolomite	-5.50	25.19	-9.42	2.75	-2.8	2.9	1567	502	-714	
Badamaqen	M. Gazhacun	W1	nod dolomite	-5.80	24.88	-9.72	2.75	-3.1	2.9	1707	544	-774	
Lower Ramaqu	M. Gazhacun	550	nod dolomite	-11.31	19.21	-15.19	2.74	-8.6	2.9	3650	1067	-1515	

(a) Mean $\delta^{18}\text{O}_w$ and associated 2 s.e.m. error calculated using WMMT of $23.8 \pm 3.4^\circ\text{C}$ (Khan and others, 2014) and calcite fractionation factor of Kim and O'Neil (1997).
 (b) Mean $\delta^{18}\text{O}_w$ and associated 2 s.e.m. error calculated using a range of lacustrine carbonates precipitation temperatures (15–30°C) and calcite fractionation factor of Kim and O'Neil (1997).
 (c) Mean $\delta^{18}\text{O}_w$ calculated and associated 2 s.e.m. using range of temperatures (MAT $8.2^\circ\text{C} \pm 10^\circ\text{C}$) for groundwater/lake sediment temperatures and fractionation factors for calcite (Kim and O'Neil, 1997), siderite (Zhang and others, 2001), and dolomite (Vasconcelos and others, 2005).
 (d) Calculated using mean low elevation Neogene $\delta^{18}\text{O}_w$ values determined from Siwalk Fm. paleosol carbonate data (Quade and Cerling, 1995; Quade and others, 2013) and low elevation WMMTs from Khan and others (2014): -6.6‰ for the Rigongla Fm. and Gazacun Gp.; -4.6‰ for the Oiyug Fm.
 (e) Derived from the sum in quadrature of the uncertainties associated with calculation of mean $\delta^{18}\text{O}_w$ values for each sample (a-c), as well as the paleotemperature ranges and corresponding carbonate fractionation factors used to determine mean low elevation Neogene $\delta^{18}\text{O}_w$ values for the Himalayan foreland (d).
 (f) Model elevation and 2 σ uncertainty calculated following the methodology detailed in Rowley and others (2001), Rowley and Garzione (2007), and Polissar and others (2009).

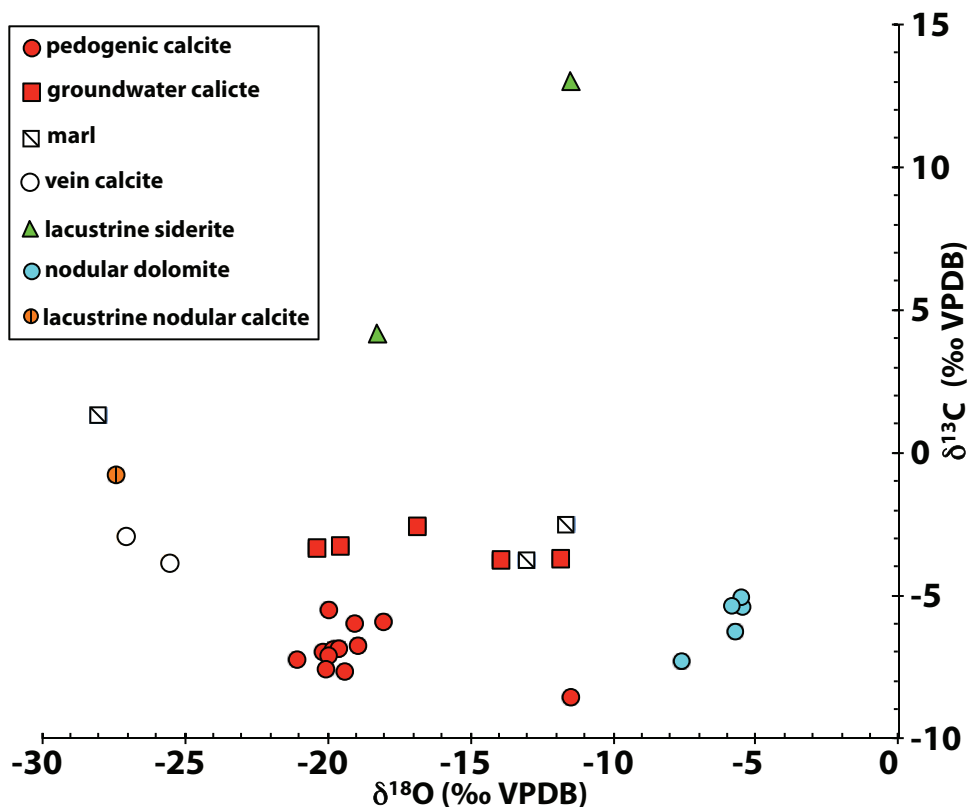


Fig. 6. $\delta^{18}\text{O}$ and $\delta^{13}\text{C}$ values for Oiyug Basin carbonates.

study were derived from the upper Gazhacun Group and the Oiyug Formation (figs. 2 and 3). Sample TAI values are equivalent to vitrinite reflectance (R_v) values of 0.3 % to 0.5 % (table B1), indicating burial temperatures ranging from 23° to 76 °C (Barker, 1988). We further assessed the thermal maturity and organic matter source of samples using sterane isomerization and the *n*-alkane odd/even preference (OEP) and average chain length (ACL) (fig. 7). Thermal maturation results in isomerization of the C_{29} sterane at C-20 from the biological 20S stereochemistry to an equilibrium mixture of the 20S and 20R isomers ($\sim 0.56 \text{ S}/[\text{S}+\text{R}]$, Peters and others, 2004). Heating and generation of petroleum *n*-alkanes will reduce the biosynthetic odd/even chain-length preference, eventually resulting in an OEP ~ 1 as the syndepositional plant-wax *n*-alkanes are overwhelmed by the petroleum source. Organic matter source can also affect the OEP as there are a range of OEP values for terrestrial vegetation, and aquatic sources can have very low OEP values. In immature sediments the *n*-alkane ACL reflects the relative input of long-chain terrestrial plant waxes and mid- and short-chain aquatic sources (macrophytes, algae). In thermally mature samples the ACL reflects oil-cracking reactions that preferentially destroy long-chain compounds and produce shorter chain homologues. Given the relatively low maturity of all samples in this study, the ACL is taken as an indicator of source.

Samples from the Oiyug Basin had C-20 S/[S+R] ratios 0.19 to 0.25 (fig. 7) indicating any burial heating occurred well below maturity levels that would alter the *n*-alkane H-isotopic composition (dos Santos Neto and Hayes, 1999; Pedentchouk and

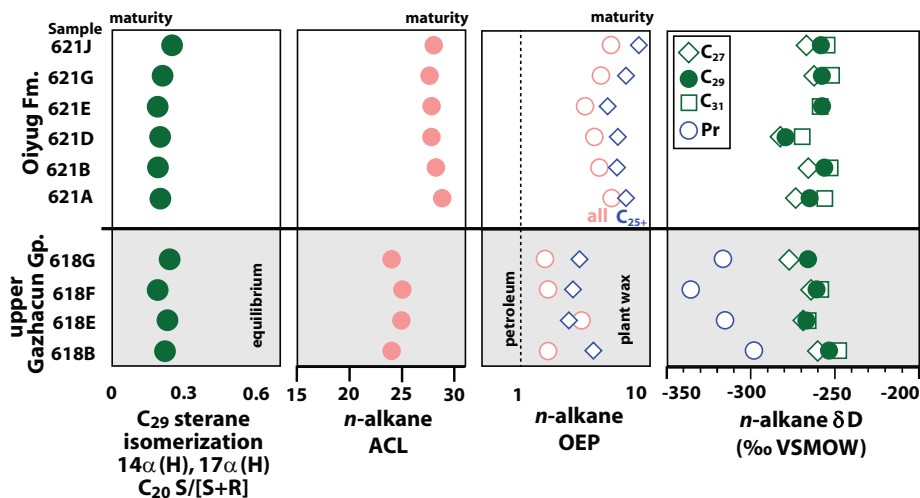


Fig. 7. Organic-molecule based thermal maturity, organic matter source, and isotopic values for upper Gazhacun Group and Oiyug Formation samples. Low thermal maturity is indicated by the predominance of the biosynthetic C_{20} S stereochemistry of the C_{29} sterane and high n -alkane average chain length (ACL) and odd/even preference (OEP). The type of vegetation also influences ACL and OEP leading to the differences observed between the upper Gazhacun Group and the Oiyug Formation. Evidence for a primary hydrogen isotope signature is further indicated by preservation of the biosynthetically-derived difference between pristane (Pr) and n -alkanes. These data indicate that long-chain, odd-carbon n -alkanes (C_{27-31}) reflect the original plant- δD signature and can be used to infer the isotopic composition of paleowaters.

others, 2006; Schimmelman and others, 2006). Oiyug Formation samples collected at the NW Oiyug section have high OEP values, also indicating minimal amounts of heating. Gazhacun Group samples have lower OEP values (1.7–3.4 for C_{11-45}) possibly indicating a contribution from petroleum n -alkanes (fig. 7). However, the OEP remains high for the C_{25+} alkanes that include the plant-wax compounds and is well within the OEP range of modern plants (Diefendorf and others, 2011; Bush and McNerney, 2013). Furthermore there is no difference in the sterane isomerization of the two formations (0.21 ± 0.02 , 0.22 ± 0.02 , $\pm 2\sigma_{\text{mean}}$) suggesting vegetation source rather than thermal maturity is responsible for the OEP differences. Pollen abundances point to modest differences in the terrestrial vegetation between the Oiyug Formation and upper Gazhacun Group (see below) that are perhaps reflected in the OEP. Also consistent with the change in OEP are differences in the n -alkane average chain length (ACL) (fig. 7). The ACL is 27.6 to 28.8 in Oiyug Formation samples indicating a dominant terrestrial vegetation source for organic matter that is consistent with identified kerogen types (table B2 and table B3). In Gazhacun Group samples, the ACL is 24.0 to 25.0 reflecting increased input from aquatic sources consistent with sample kerogen content (table B3). Input of mid- and short-chain algal or macrophyte n -alkanes with low OEP may be responsible for the lower OEP in these samples. Generally it appears the Oiyug Formation is dominated by terrestrial vegetation while the Gazhacun Group includes inputs of short-chain n -alkanes from aquatic sources distinct from the long-chain plant-waxes also present.

Overall, the molecular data indicate low thermal maturity and preservation of the original n -alkane δD composition. This assessment is supported by preservation of the biosynthetically derived hydrogen isotope difference between lipid groups in these samples. The δD value of pristane is -40 to -80‰ more negative relative to the C_{19} and C_{21} n -alkanes. This offset reflects the lower δD values of isoprenoid relative to

acetogenic lipids imprinted during biosynthesis (Pedentchouk and others, 2006; Schimmelmann and others, 2006). Thermal maturation erases this difference, therefore the observed offset provides further support for preservation of the primary hydrogen isotope values in these samples.

Lipid and water δD values.—Hydrogen isotope values for C_{25+} odd-carbon n -alkanes range between -285 and -235 permil VSMOW (table B4). There is a ~ 20 permil range within each homologue and no systematic differences in values between formations. Isotope values are most negative for C_{25} (or C_{23} if present) and increase by 4 to 7 permil for each additional two carbons, reflecting biosynthetic effects during chain elongation (Chikaraishi, and others, 2004) and/or perhaps varying proportions of different plant sources. Even carbon number homologues exhibit more positive δD values compared to adjacent odd-carbon homologues for C_{23+} n -alkanes consistent with their different biosynthetic precursor (Zhou, and others, 2010b) further indicating preservation of the original hydrogen isotope values.

Calculated meteoric water δD composition from lipid δD .—Studies of modern plants, soils and sediments indicate the primary control on plant-wax δD is the isotopic composition of rainfall and isotopic fractionation during lipid biosynthesis (Sachse and others, 2012). Important secondary controls include vegetation type and the evaporative enrichment of deuterium in soil and leaf waters (Polissar and Freeman, 2010; McInerney and others, 2011; Sachse and others, 2012). The effects of biosynthesis and vegetation type are encapsulated in an “apparent” fractionation factor that relates the hydrogen isotopic composition of a lipid molecule to the source water used by a plant:

$$\epsilon_a = [(\delta D_{\text{lipid}} + 1) / (\delta D_{\text{water}} + 1)] - 1 \quad (1)$$

Values for ϵ_a are determined empirically based upon analysis of lipids in modern plants or sediments and measurement or inference of their source water (usually rainfall). At present, the essential differences in ϵ_a appear to reflect broad groupings of plant functional type (trees, forbs, shrubs and grasses) and photosystem (C_3 , C_4 , CAM) (McInerney, and others, 2011; Sachse and others, 2012).

Here we use pollen abundances to infer the dominant plant functional types and appropriate ϵ_a values for our samples. Pollen from the Oiyug Formation indicates a dominantly woody tree/shrub environment, with grass pollen detected in trace amounts from only one sample (fig. 8). Organic samples from the upper Gazhacun Group are dominated by gymnosperm pollen with lesser abundances of angiosperms. Gazhacun samples were devoid of grass pollen (fig. 8). Floral macrofossils from the same stratigraphic interval as our samples indicate the existence of a boreal temperate broad-leaved deciduous forest dominated by angiosperms (Khan and others, 2014). Additionally, pedogenic carbonate $\delta^{13}C$ values from the upper/lower Gazhacun Group and the underlying Rigongla Formation average -5.52‰ to -8.58‰ , with a mean of -6.9‰ ($n=15$). These values are generally consistent with pedogenic calcite formation in the presence of C_3 vegetation in soils with low soil respiration rates (Quade and others, 1989). Overall these data indicate a C_3 -dominated ecosystem in both formations with no significant amounts of grassland cover throughout the depositional history of the Oiyug Basin.

We use the δD of C_{29} n -alkanes to infer precipitation δD because most modern calibration studies have focused on this molecule. Based upon the paleovegetation data we use an ϵ_a value of $-111 \pm 30\text{‰}$ (2σ) calculated from modern C_3 dicotyledonous angiosperm and gymnosperm trees and shrubs (McInerney, and others, 2011; Sachse and others, 2012).

Calculated paleoprecipitation δD values for plant wax samples from the middle Miocene upper Gazhacun Group range from -175‰ to -161‰ , with a mean of $-170 \pm 7\text{‰}$ (± 2 s.e.m.) (table 4). Similarly, calculated paleoprecipitation δD values

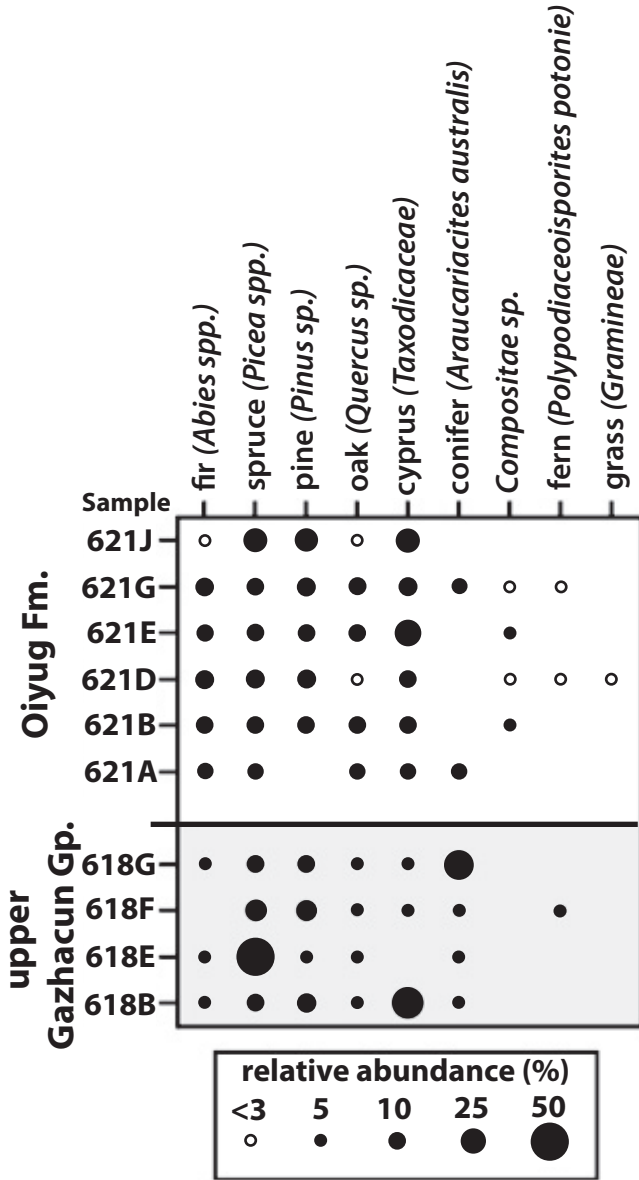


Fig. 8. Pollen abundances from Namling-Oiyug upper Gazhacun Group and Oiyug Formation organic samples.

for samples from the late Miocene-Pliocene Oiyug Formation range from between -164‰ and -190‰ with a mean of $-171 \pm 8\text{‰}$ (table 4). The absolute uncertainty in this value on the VSMOW scale is $\sim \pm 30\text{‰}$ (2σ) (table 3, table B4), principally reflecting the range in ϵ_a values in modern plant calibration datasets (Polissar and D’Andrea, 2014). The inferred rainfall δD values are about -20 permil more negative than modern water from the Oiyug Basin (-150‰ VSMOW, Currie and others, 2005), however this difference becomes ~ 10 permil after accounting for changes in seawater

TABLE 3
Upper Gazhacun Group and Oiyug Formation sample lipid and paleometeoric water δD values and calculated paleoelevations

Sample	Unit	lithology	$\delta D_{C_{29}}$ (‰ vsmow)	$\epsilon_{C_{29},water}$ (‰)	δD_w (‰ vsmow)	2σ (\pm ‰)	mean $\delta D_{low-elev}$ (‰ vsmow)	2 s.e.m. (\pm ‰)	$\Delta\delta D_w$ (‰ vsmow)	$\Sigma \Delta\delta D_w$ Uncertainty	model paleoelevation (m)	2 σ model error (\pm m)	2 σ model error (-m)
			(a)	(b)	(c)	(d)	(e)	(f)	(g)	(h)	(i)	(j)	(k)
621J	Oiyug	mudstone	-258	-111	-166	31	-27	3	-143	31	5359	1435	-2094
621G	Oiyug	shale	-258	-111	-166	31	-27	3	-142	31	5354	1434	-2092
621E	Oiyug	mudstone	-258	-111	-165	31	-27	3	-142	31	5347	1433	-2090
621D	Oiyug	mudstone	-280	-111	-190	30	-27	3	-167	31	5827	1516	-2278
621B	Oiyug	mudstone	-256	-111	-163	31	-27	3	-140	31	5312	1427	-2078
621A	Oiyug	mudstone	-265	-111	-173	30	-27	3	-150	31	5511	1461	-2150
618G	U. Gazhacun	mudstone	-266	-111	-174	30	-43	3	-137	31	5252	1416	-2057
618F	U. Gazhacun	mudstone	-261	-111	-169	31	-43	3	-132	31	5136	1397	-2019
618E	U. Gazhacun	shale	-267	-111	-175	30	-43	3	-138	31	5275	1420	-2065
618B	U. Gazhacun	shale	-254	-111	-161	31	-43	3	-123	31	4968	1369	-1966

(a) Calculated δD_w uncertainty associated with the range in ϵ_a values in modern plant calibration datasets and analytical uncertainty (Polissar and D'Andrea, 2014).
 (b) Mean $\delta D_{low-elev}$ and ± 2 s.e.m errors derived from Siwalk Fm, paleosol carbonate $\delta^{18}O_w$ values (Cerling and Quade, 1995; Quade and others, 2014) calculated for a range of low elevation WMMTs from Khan and others (2014). $\delta^{18}O_w$ values were converted to δD_w using modern $\delta D-\delta^{18}O$ relationships in meteoric water (Rozanski and others, 1993).
 (c) Derived from the sum in quadrature of the uncertainties associated with calculation of δD_w (a) and mean $\delta D_{low-elev}$ (b) values for each sample.
 (d) Model elevation and 2 σ uncertainty calculated following the methodology detailed in Rowley and others (2001) and Rowley and Garzzone (2007), and Polissar and others (2009).

δD since the early Neogene (Billups and Schrag, 2003). This difference is well within the uncertainty of lipid-based water compositions and suggests no significant shift in precipitation values since the Miocene.

PALEOALTIMETRY OF THE OIYUG BASIN

Stable Isotope Paleoaltimetry

In a rising parcel of air, the stable isotopic composition of precipitation changes systematically with altitude due to progressive distillation of water vapor during condensation. This “altitude effect” can be modeled as an open-system Rayleigh distillation with a temperature-dependent isotopic fractionation factor (Rowley and others, 2001; Rowley and Garzzone, 2007). If the isotopic composition of meteoric water at a particular location is known, the altitude of that location can be estimated using theoretical and empirically derived functions for changes in the isotopic composition of precipitation with respect to altitude.

In this study, paleoelevations for the late Oligocene to Pliocene Oiyug Basin are calculated from the difference between the isotopic composition of high- and low-elevation precipitation ($\Delta\delta$) following the methodology detailed in Rowley and others (2001) and Rowley and Garzzone (2007), and modified by Polissar and others (2009). At present there are no Oligocene estimates of low elevation precipitation in the foreland of the Himalayas, so we use estimates derived from the Miocene and Pliocene discussed below. The Neogene isotopic composition of low-elevation precipitation in the Himalayan foreland is inferred from the isotopic compositions of soil carbonate nodules ($\delta^{18}\text{O}_c$) in the middle Miocene Siwalik Formation (~14–17 Ma) in Pakistan [$-9.5 \pm 0.8\text{‰}$ (± 2 s.e.m.) VPDB; Quade and Cerling, 1995] and upper Miocene-Pliocene Siwalik Formation (5.9–4.7 Ma) in Nepal [$-7.5 \pm -0.6\text{‰}$ (VPDB); Quade and others, 2013]. As pedogenic carbonates in the modern Himalayan foreland form during the warmest times of the year (Quade and others, 2013), the isotopic composition of the meteoric water from which they precipitate can be estimated by considering warm month mean temperature (WMMT) from other proxy data. Recent fossil leaf physiognomic studies from the Siwalik Group of northern India indicate the WMMT values of 27.84 ± 3.39 °C and 28.35 ± 3.39 °C for the middle Miocene, and 28.14 ± 3.39 °C for the late Miocene-Pliocene (Kahn and others, 2014). This temperature is within error of calculated calcite ‘clumped’ isotope Δ_{47} precipitation temperatures for the Miocene-Pliocene pedogenic carbonates from Nepal (29.7 ± 6.5 °C; Quade and others, 2013). Using the mean fossil floral-derived Neogene WMMT temperatures and their error ranges, the pedogenic $\delta^{18}\text{O}_c$ values from the Himalayan foreland indicate a middle Miocene low-elevation $\delta^{18}\text{O}_w$ composition of $-6.6 \pm 0.3\text{‰}$ (± 2 s.e.m.) VSMOW, and a Miocene-Pliocene low-elevation $\delta^{18}\text{O}_w$ composition of $-4.6 \pm 0.4\text{‰}$ VSMOW.

The δD of low elevation Miocene precipitation can be estimated by using the Miocene low-elevation $\delta^{18}\text{O}_w$ composition to calculate a corresponding δD value using the modern global meteoric water line (Rozanski and others, 1993). Using this relationship, the δD of low elevation precipitation used in our calculations is $-43 \pm 3\text{‰}$ (± 2 s.e.m.) for the middle Miocene, and $-27 \pm 3\text{‰}$ for the Miocene-Pliocene.

Note that for the hydrogen isotope system we calculate the difference between high- and low-elevation samples as a fractionation rather than an arithmetic difference using the equation:

$$\Delta\delta\text{D} = [(\delta\text{D}_{\text{water}} + 1)/(\delta\text{D}_{\text{low-elev}} + 1)] - 1 \quad (2)$$

This is necessary because isotopic fractionations such as condensation and air mass rainout act upon relative, rather than absolute, isotopic ratios. The isotopic depletion with altitude occurs through a series of fractionation steps such that the isotope-

elevation relationship is controlled by the magnitude of net isotopic fractionation, not the net arithmetic difference. This distinction is inconsequential for the O isotope system where the isotope value of low-elevation rainfall is less than 1 percent from the zero point of the isotopic scale. However, for the H isotope system, the isotope value is 3 to 4 percent less than the zero point of the isotopic scale and the arithmetic difference, if applied, would be systematically in error.

Consideration of Uncertainties

Uncertainties in our paleoaltimetry estimates derive from several sources. First is the uncertainty in the isotopic compositions of water calculated for our samples and for the composition of low-elevation meteoric water. This includes the uncertainty in the temperature of precipitation for carbonates and the uncertainty in the apparent fractionation for leaf wax molecules. These values are readily calculable and are reported here in table 2 and table 3. Second is the uncertainty in how reconstructed water compositions are affected by evaporation. Evaporation, particularly from lakes and arid soils can significantly increase the isotopic composition of surface waters yielding erroneously low calculated elevations. Comparing water compositions from different evaporative systems such as leaf-waxes, lacustrine calcite, and pedogenic carbonates can assess this uncertainty (Polissar and others, 2009). As discussed above, it is evident from our data that significant evaporative enrichment has occurred in some samples, particularly from the middle Miocene Gazhacun Group. This is consistent with the findings by Polissar and others (2009) from other large lakes on the Tibetan Plateau at this time. In these samples, the more depleted isotope values will be closer to the true meteoric water composition and provide better paleoaltimetry estimates (Polissar and others, 2009). For this reason, samples with relatively high $\delta^{18}\text{O}$ values ($> -10\text{‰}$) are excluded from the paleoelevation estimates.

A third uncertainty is natural variability in the $\delta^{18}\text{O}$ of meteoric precipitation. At high elevations this isotopic variation typically is also reflected in contemporaneous variations at low elevation (Gonfiantini and others, 2001). By their very nature the measured samples likely represent multi-decadal and greater time averages that significantly dampen large amplitude annual variability typically seen in precipitation data (Gonfiantini and others, 2001) and ice-cores (Thompson and others, 2000). The reported isotopic values therefore more closely match the long-term mean isotopic compositions that are modeled in paleoaltimetry calculations. Further averaging of isotope values from multiple samples effectively removes this effect by computing population means from low- and high-elevation sites. We take this approach here, calculating the mean and standard error of the mean for water isotope values for Oiyug Basin stratigraphic intervals and from Miocene low elevation sites from the Himalayan foreland basin. The difference between these values ($\Delta\delta\text{D}$ and $\Delta\delta^{18}\text{O}$) is used in the paleoelevation model calculations. Errors for the $\Delta\delta$ values are derived from the sum in quadrature of the uncertainties associated with carbonate fractionation factors using the range of paleo temperatures described above for each proxy (table 4).

The fourth and final source of uncertainty is the relationship between isotopic composition and elevation (the isotopic lapse rate). The isotopic lapse rate systematically depends upon temperature and humidity and can be calculated numerically (Rowley and others, 2001). However, the temperature and humidity of low-elevation airmasses in the past have considerable uncertainty that can affect paleoelevation estimates. Here we follow the approach in Rowley and others (2001) to use a large range of temperature and humidity values that reflects their modern joint probability distribution in tropical and subtropical oceanic regions. We further discuss the effects of known Cenozoic changes in global and tropical temperatures on our elevation estimates (see below).

TABLE 4
Oiyug Basin Mean Paleoelevations

Formation	Age	Mean	± 2 s.e.m.	Mean	$\Sigma \pm 2$ s.e.m.	Model Elevation (m)	2 σ Model Uncertainty (+m/-m)
		$\delta^{18}\text{O}_w$ (‰)	(‰)	$\Delta\delta^{18}\text{O}_w$ (‰)	(‰)		
		(a)	(b)	(c)	(d)	(e)	
Oiyug Fm.	~5 Ma	-22.40	1.59	-17.8	1.8	5509	+1390/-1993
upper Gazhacun Gp.	~15 Ma	-22.16	1.09	-15.6	1.4	5136	+1339/-1913
upper Ringonla Fm./ lower-middle Gazhacun Gp.	~31-16 Ma	-15.30	0.57	-10.2	1.0	4057	+1154/-1640

(a) Mean calculated from $\delta^{18}\text{O}_w$ values listed in table 2. Includes $\delta^{18}\text{O}_w$ values converted from organic [i]n[r]-alkane δD_w values listed in table 3 using modern δD - $\delta^{18}\text{O}$ relationships in meteoric water (Rozanski and others, 1993).

(b) ± 2 standard error of the mean derived from the range of $\delta^{18}\text{O}_w$ values calculated from each sample using carbonate fractionation factors and the range of paleotemperatures described in the text for each carbonate proxy, as well as the range of $\delta^{18}\text{O}_w$ values converted from the organic δD_w values listed in Table 3 given the ± 30 - 31 ‰ uncertainty associated with those samples.

(c) Represents the difference between mean $\delta^{18}\text{O}_w$ values for each Oiyug Basin interval (a) and mean low elevation Neogene $\delta^{18}\text{O}_w$ values determined from Siwalk Fm. paleosol carbonate data (Quade and Cerling, 1995; Quade and others, 2013) and low elevation WMMTs from Khan and others (2014): -6.6‰ for the Rigongla Fm. and Gazacun Gp.; -4.6‰ for the Oiyug Fm.

(d) Derived from the sum in quadrature of the uncertainties associated with calculation of mean $\delta^{18}\text{O}_w$ values for each Oiyug Basin stratigraphic interval (b), as well as the paleotemperature ranges and corresponding carbonate fractionation factors used to determine mean low elevation Neogene $\delta^{18}\text{O}_w$ values for the Himalayan foreland.

(e) Model elevation and 2 σ uncertainty calculated following the methodology detailed in Rowley and others (2001) and Rowley and Garzzone (2007), and Polissar and others (2009).

Paleoaltimetry Results

Using the difference between estimated Neogene low-elevation meteoric isotopic compositions from the Himalayan foreland and those from the Oiyug basin, calculated Oligocene and early-middle Miocene (<31–15 Ma) paleoelevation estimates from Rigongla Formation and lower/middle Gazhacun Group carbonates range from ~3650 to 5000 m (table 2), with a mean elevation of 4057 +1154/–1640 m (2 σ) (fig. 9; fig. 10; table 4). Lacustrine marls/dolomite nodules and pedogenic carbonates with relatively high $\delta^{18}\text{O}_w$ values ($\Delta\delta^{18}\text{O}_w > -5.0$ ‰) from the middle part of the Gazhacun Group likely precipitated from evaporatively enriched meteoric waters and thus are excluded from the calculations.

Calculated paleoelevations from δD values for plant wax samples from the ~15 Ma upper Gazhacun Group range from 4968 m to 5252 m, with a mean of 5148 +1400/–2027 m. A siderite-derived paleoelevation for the same interval yielded a similar value of 5038 m +1325/–1892 m. Collectively, the mean paleoelevation for the interval is 5136 m +1339/–1913 m (2 σ) (fig. 10; table 4).

Late Miocene-Pliocene (~5 Ma) calculated paleoelevations for samples from the Oiyug Formation range from ~3900 m to ~6300 m. Calcite-derived calculated paleoelevations from Oiyug Formation lacustrine marl and carbonate nodules are 6080 m +1480/–2104 m and 6332 m +1486/–2143 m, respectively. The δD -based paleoelevation estimates from organics in the same succession range from 5827 m to 5347 m, with a mean of 5452 m +1451/–2131. The $\delta^{18}\text{O}$ value of siderite from the same section is more positive (likely reflecting evaporative enrichment of lake waters and associated shallow pore fluids) resulting in a lower paleoelevation estimate of 4026 m +1148/–1631 m. Collectively, the mean paleoelevation for the sample interval is 5509 m +1390/–1993 m (2 σ) (fig. 10; table 4).

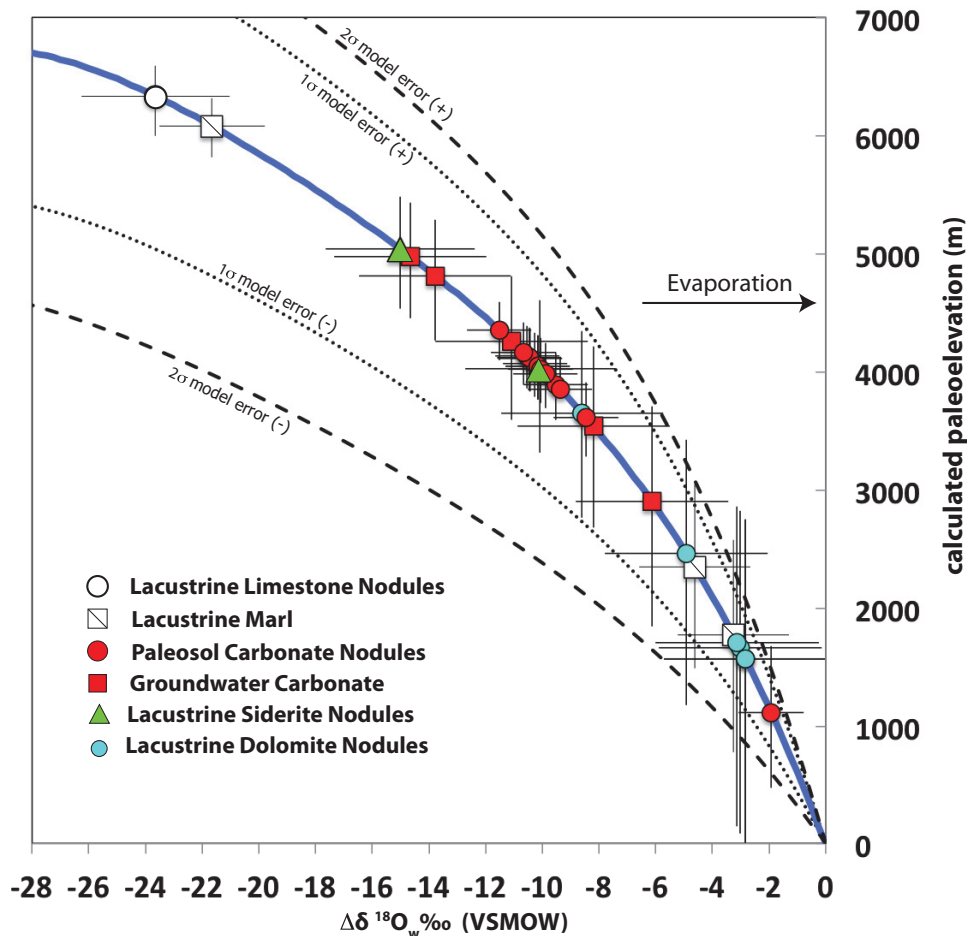


Fig. 9. $\Delta\delta^{18}\text{O}_w$ versus predicted elevations derived from Oiyug Basin carbonates with the model curve from Rowley and others (2001) shown for reference. Two sets of uncertainties are plotted with each data point. Horizontal error bars reflect the range of $\delta^{18}\text{O}_w$ compositions given the range of environmental temperatures used in calculating carbonate/water fractionation factors. These uncertainties give rise to an uncertainty in the estimate of the mean elevation of the sample, shown by the black vertical bars. Dashed and dotted lines reflect 2σ and 1σ model uncertainties associated with starting relative humidity and temperature of low elevation moisture sources. Arrow shows the expected influence of evaporation on predicted elevation.

DISCUSSION

The calculated mean paleoelevations for the Oiyug basin indicate an overall increase in paleoelevation from ~ 4.1 km in the late Oligocene-early Miocene (~ 31 – 16 Ma), ~ 5.1 km for the mid-Miocene (~ 15 Ma), and ~ 5.5 km for the late Miocene-Pliocene (~ 5 Ma). It should be noted, however, that the apparent ~ 1.4 km increase in elevation between early and late Miocene time is within the 1.2 to 2 km error associated with the model calculations. As a result, paleoelevations may have remained relatively unchanged throughout late Paleogene-Neogene deposition in the basin. In addition, changes in tropical temperatures could affect this result through their control of the isotopic lapse rate. Estimates of tropical and subtropical ocean temperatures from non-upwelling regions indicate a broad decrease from the Paleogene through the

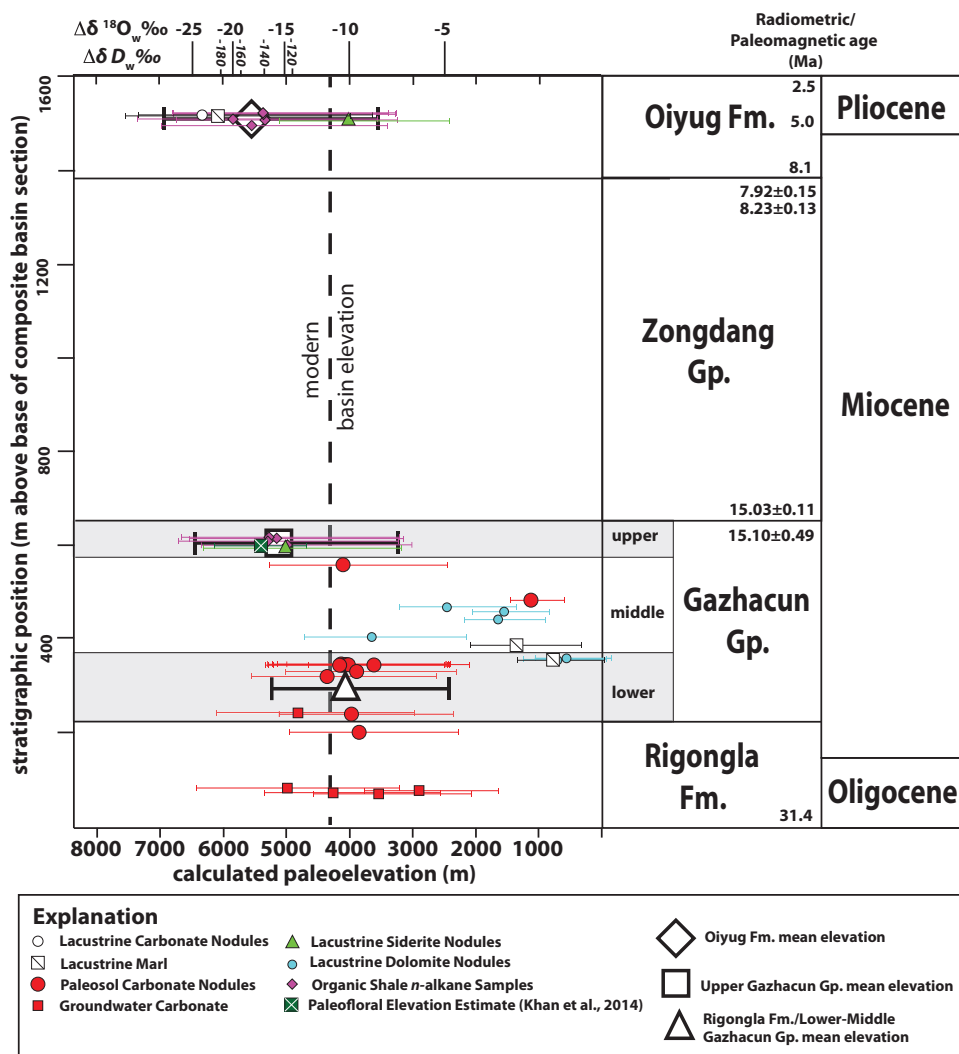


Fig. 10. Time-stratigraphic $\Delta\delta D$ and $\Delta\delta^{18}O$ and model paleoelevation and 2σ model error estimates for carbonate and organic samples from the Oiyug basin. Carbonate samples with $\Delta\delta^{18}O$ values that are likely evaporatively enriched ($> -5\text{‰}$) and were not included in mean elevation calculations for the Rigongla Formation/lower-middle Gazhacun Group, upper Gazhacun Group, and Oiyug Formation stratigraphic intervals. The fossil-floral physiognomic paleoelevation of $5.4 \text{ km} \pm 0.7 \text{ km}$ for the upper Gazhacun Group of Khan and others (2014) is shown for comparison.

Neogene of 0 to -4 C (Stewart and others, 2004; LaRiviere and others, 2012; Zhang and others, 2013; Zhang and others, 2014) that would increase the isotopic lapse rate. Inclusion of these temperature changes would yield higher model paleoelevations in the Neogene than those using the modern calibration (Rowley, 2007). Warmer Oligocene-middle Miocene temperatures compared to those in the late Miocene and Pliocene would also result in calculated Oligocene-Middle Miocene elevations that are closer to the Miocene-Pliocene elevations. Importantly for our purposes, even if late Paleogene and Neogene tropical sea-surface temperatures were as much a $5 \text{ }^\circ\text{C}$ warmer than today, the model paleoelevations would be no more than $\sim 1 \text{ km}$ higher than our

calculated values. This difference falls well within our current range of uncertainty and does not affect the conclusions presented here.

The overall uncertainty of the calculated paleoelevations can be evaluated in a relative sense by comparing the results from different paleoaltimetry proxies from the same stratigraphic interval. For example, the range of calculated paleoelevations from plant wax δD for the ~ 15 Ma upper Gazhacun Group (~ 5.0 - 5.3 km) are similar to paleoelevation estimates of 5.4 ± 0.7 km based on Oiyug basin fossil floral physiognomy from the same interval (Kahn and others, 2014) (fig. 10). In addition, these estimates overlap within uncertainty with the siderite-derived paleoelevation of ~ 5.0 km from the same stratigraphic zone (fig. 10). The close agreement of these different paleoelevation proxies provides an additional degree of confidence in the fidelity of the calculated elevations. When considering the potential for isotopic variations related to original basin hydrological conditions and variable carbonate precipitation temperatures, that the calculated paleoelevations overlap within uncertainty throughout the sample suite provides further support of overall study results.

Given that the mean elevations for the Oligocene-Pliocene Oiyug basin fall close to or above the present-day basin-floor elevation of ~ 4300 m and that inferred water isotopic values are more negative than modern Oiyug basin waters (Currie and others, 2005), the first order conclusion of our investigation is that the southern part of the Tibetan Plateau has remained at high elevations since at least the late Oligocene (~ 31 Ma).

The timing of development of high topography across the Himalayas and Tibet remains an important and open question. Recent results from the Paleocene-Eocene Penbo/Linzhou Basin based on $\delta^{18}O_c$ (Ding and others, 2014) and combined clumped isotopes paleothermometry and $\delta^{18}O_c$ (Ingalls and others, in review¹) have been interpreted to imply that at least parts of the Lhasa block may have been at relatively high-elevations ($\sim >4000$ m) since ~ 55 Ma. Previous studies from the Penbo region, however, have interpreted relatively low $\delta^{18}O$ values from pre-Cenozoic nonmarine carbonates as reflecting substantial diagenetic resetting of the oxygen isotopes associated with high temperature (>50 °C) alteration, leaving the Ding and others (2014) results intriguing but in need of further confirmation (Leier and others, 2009). Ingalls and others (in review) highlight the existence of both high temperature (>40 °C) and low temperatures (~ 10 °C) calcites from this region, but emphasize that they record comparable $\delta^{18}O_c$, irrespective of temperature and thus imply alteration in a rock-dominated system.

Polissar and others (2009) confirmed and extended the results of Rowley and Currie (2006) from the Lunpola Basin, by showing an absence of organic thermal maturation of these samples, and that the most negative $\delta^{18}O_c$ and compound-specific δD values fall on the meteoric water line and hence are internally consistent. The Lunpola data imply high (>4 km) elevations for central Tibet from at least Oligocene and perhaps late Eocene based on paleontological estimates of the ages of the sampled units (Rowley and Currie, 2006). Hoke and others (2014) added data from the southeastern margin of the Tibetan Plateau in Yunnan where they derive paleoelevation estimates for late Eocene pedogenic carbonates of the Liming Basin that are comparable with the current elevation of ~ 2700 m. More recently Li and others (2015) report additional isotope-based paleoaltimetry estimates from eastern Tibet that support paleo-elevations comparable to present for the Markham and Jianchuan basins for sequences thought to be ~ 23 to 16 Ma in age. Interestingly the age of the Jianchuan Basin fill has been revised based on both U-Pb dates on zircons (35 – 38 Ma)

¹ Ingalls, M., Rowley, D., Currie, B., Li, S., Olack, G., Ding, L., and Colman, A. L., in review, Paleocene-early Eocene high elevation of the Linzong arc implies large-scale subduction of continental crust during Himalayan collision: Nature Geoscience.

and fossils of Late Eocene age (Gourbet and others, 2015). This implies little change in elevation of at least the Jianchuan basin since the Late Eocene.

DeCelles and others (2007) calculated stable-isotope based paleoelevations similar to modern elevations for the Oligocene Nima Basin in central Tibet. Although, recent work by Huntington and others (2015) identified potential high-temperature (>50 °C) alteration in Nima lacustrine carbonates, the authors concluded that alteration occurred under rock-buffered conditions that preserved original carbonate isotopic compositions. As such, the DeCelles and others (2007) paleoelevation estimates of > 4.5 Km for the Nima region at ~26 Ma likely remain valid.

Paleoaltimetry estimates from the Oiyug basin are consistent with elevations at least as high as present throughout the past ~31 Ma. The results presented above add to an expanding array of paleoaltimetry data from southern Tibet and the High Himalayas compatible with high elevations persisting there from at least 20 Ma (France-Lanord and others, 1988). For example, G ebel and others (2013) presented δD -derived paleoelevation estimates of >5000 m from ~16 Ma hydrothermally altered hydrous minerals (biotite and hornblende) from the South Tibetan Detachment, from just north of Mount Everest. Huntington and others (2015), significantly augmented the work of Saylor and others (2009) with clumped-isotope paleotemperature data, calculated paleoelevations of ~5.4 km from ~8.5 to 3.7 Ma deposits in the Zhada Basin in southwestern Tibet. These studies complement earlier estimates from Gyrong (Rowley and others, 2001), and Thakkhola (Garziona and others, 2000; Rowley and others, 2001) that indicate paleoelevations along the southern margin of the Plateau of >5 km since ~10 Ma.

Collectively, existing paleoaltimetry data from the southern and central Tibetan Plateau imply that elevations have remained at close to modern-day elevations since at least late Eocene-Oligocene time over a region at least as far southeast as the Liming Basin in Yunnan. These studies support previous interpretations implying no demonstrable large-scale role of convective destabilization of the Tibetan lithospheric mantle, at least within this time interval. Models invoking very large-scale contributions of mantle lithospheric loss driving increased elevations *ca.* 8 Ma (Molnar and others, 1993) are at odds with these data. Smaller-scale contributions from mantle lithospheric drips (Molnar and Stock, 2009) remain possible, but are small enough so that they are not testable with existing paleoaltimetry data. Overall, these results imply that crustal thickening is likely the dominant control on elevation in this collisional regime (Rowley and Currie, 2006). Additionally, our results allow for a possible increase in elevation from 4.0 km to 5.5 km between early and late Miocene time with a subsequent decrease towards the present, as has been suggested elsewhere (Saylor and others, 2009). Given that the modern elevation of the Oiyug basin floor is ~4300 m, it is possible that elevations in part of the Tibetan Plateau have decreased by >1 km since the early Pliocene (Khan and others, 2014). This result is similar to interpretations of a possible 1 to 1.5 km decrease in the elevation of the Zhada Basin in western Tibet since the late Miocene (Saylor and others, 2009; Huntington and others, 2015), and is compatible with widespread east-west extension in Tibet since that time (Harrison and others, 1995; Hurtado and others, 2001).

CONCLUSIONS

Stable isotope-based estimates of paleoelevation for the Oiyug Basin in south central Tibet indicate the region has been at elevations in excess of 4 km since ~31 Ma. Oligocene and early-middle Miocene (<31–16 Ma) $\delta^{18}O$ paleoelevation estimates from groundwater and pedogenic carbonates indicate basin elevations of elevation of ~4.1 km. Measured δD values from plant wax *n*-alkanes and lacustrine-siderite $\delta^{18}O$ compositions sampled from middle Miocene (~15 Ma) strata indicate elevations of ~5.1 km. This estimated elevation is similar to the 5.4 km paleoelevation estimate

based on fossil-floral physiognomy from the same sample locality (Kahn and others, 2014). Calculated late Miocene-Pliocene paleoelevation estimates derived from the $\delta^{18}\text{O}$ composition of lacustrine marls and carbonate/siderite concretions, as well as the δD of plant wax *n*-alkanes indicate a mean elevation of ~ 5.5 km at ~ 5 Ma.

Although calculated mean paleoelevations for the Oiyug basin all fall within the 1.2 to 2 km errors associated with the model calculations, the close agreement of the different paleoelevation proxies (calcite/siderite/dolomite $\delta^{18}\text{O}$, *n*-alkane δD , and fossil-floral physiognomy) presented and discussed above provides an additional degree of confidence in the fidelity of the calculated elevations. As such, the results of our study allow for a possible increase in Oiyug basin elevation from 4.1 km to 5.5 km during the early and late Miocene, followed by a >1 km decrease in elevation since the early Pliocene. These findings, as well as those of other Tibetan paleoaltimetry studies, are consistent with tectonic models where the Tibetan Plateau has remained high since at least the initiation of India-Asia collision during the Eocene, and subsequent late Cenozoic extensional collapse.

ACKNOWLEDGEMENTS

We are grateful to Albert Colman at the University of Chicago, David Dettman at the University of Arizona, and Daniel Schrag at Harvard University for the stable isotope analyses reported in this paper. We also thank Gerald Waanders for analyzing our organic samples and compiling the presented palynological data. Reviews by Joel Saylor, Ding Lin, and the AJS Associate Editor greatly improved the quality of the manuscript. We also thank Erchie Wang, Institute of Tibetan Research, Chinese Academy of Sciences, and Chengshan Wang, China Geosciences University for arranging field access and logistical support, and William Wilcox for assistance in the field. This work was funded by National Science Foundation grants to Currie (EAR-0609756), Rowley (EAR-0609782; EAR-1111274), and Albert Colman and Rowley (EAR-0923831). Postdoctoral funding for Polissar was provided by the Canadian Institute for Advanced Research-Earth System Evolution Program.

APPENDIX A. METHODS

Carbonate Samples

Sample preparation.—Carbonate samples for XRD analysis were obtained from thin section billets or from polished slabs using a small chisel. Powdered samples for isotopic analysis were obtained using a dental drill on thin-section billets to directly determine the micromorphology of sampled material. The mineralogical composition of collected samples was confirmed by X-ray powder diffraction, using CuK α radiation, on a Sintag powder diffractometer at Miami University.

Carbonate isotopic analyses.—Samples were analyzed at the University of Arizona, Harvard University, and the University of Chicago. At the University of Arizona, 0.2 mg of each sample were heated at 150 °C for 3 hours in vacuo and processed using an automated sample preparation device (Kiel III) attached directly to a Finnigan MAT 252 mass spectrometer. Values were normalized to NBS-19 based on internal lab standards and precision of repeated standards is $\pm 0.1\%$ for $\delta^{18}\text{O}$ and $\pm 0.06\%$ for $\delta^{13}\text{C}$ (1 σ). At Harvard University, approximately 2 mg of bulk sample was loaded into a stainless steel vial and dried in an oven at 50 °C for 48 hours. Samples were dissolved on line in a common acid bath of orthophosphoric acid at 90 °C. Precision (1 σ) averages 0.07‰ for $\delta^{18}\text{O}$ and 0.05‰ for $\delta^{13}\text{C}$.

At the University of Chicago, approximately 0.3 to 0.5 mg of powdered sample was added to an Exetainer tube, sealed, and flushed with helium. 0.1ml of nominally 103% phosphoric acid was injected into the flushed Exetainer tubes for carbonate digestion. Calcite was digested at 26 °C overnight on the gas bench. Iron-bearing carbonates were prepared separately to accommodate for higher temperature and longer digestion times. Multiple tests were done on in house siderite standards and NBS-18 and NBS-19 calcite standards to test for $-\text{CO}_3^{2-}$ yield during different modes of digestion. The calcite standards had $\sim 100\%$ yield when reacted with phosphoric acid at 26 °C for >12 hours. Under the same conditions, siderite sample 618A had $\sim 2\%$ carbonate yield. Approximately 80% reacted after two days at 60 °C, assuming 618A is pure iron carbonate. Fe-carbonate sample powder was added to Exetainer tubes, flushed with helium, and set horizontally in a 60 °C drying oven. The glass bottom of the Exetainer tube was lifted to a low angle, allowing for the sample to sit above the height of the Exetainer cap, but low enough that the sample powder could not slip to the lower height of the cap and react with the acid. 103% phosphoric acid was carefully

added by syringe through the cap so the acid would pool below the sample powder out of contact. Once acid and powder were at temperature, the vials were put in a vertical position to allow the acid to react with the carbonate. Calcium and iron carbonate samples were analyzed on a Thermo Delta V Plus interfaced with a GasBenchII. NBS-19 was digested at 60°C over six days with multiples of 618A and 621F so these data could be corrected to a standard treated under the same conditions. Multiple NBS-18 and NBS-19 were digested at 60°C overnight and analyzed on the same day as the standard and samples under the six day treatment. Corrections were done to the NBS 18 and 19 standards, and appropriate fractionation factors were applied to the data depending on mineralogy and reaction temperature (see table A1 below). The precision for the siderite samples (1σ , $n=4$) was ± 0.12 and ± 0.24 per mil for $\delta^{13}\text{C}$ and $\delta^{18}\text{O}$ respectively. The oxygen isotopic value of the carbonate ($\delta^{18}\text{O}_{\text{carbonate}}$) was converted to the oxygen isotopic value of the formation water ($\delta^{18}\text{O}_{\text{w}}$) using mineralogy-specific fractionation factors listed below, where T is the reaction temperature (T_{rxn} , 333K or 299K) for carbonate-acid derived CO_2 or formation temperature for carbonate-water fractionation (T_{fm}).

$$\alpha_{\text{carb,CO}_2\text{-acid}} = \frac{1000 + \delta^{18}\text{O}_{\text{CO}_2, \text{acid}}}{1000 + \delta^{18}\text{O}_{\text{carbonate}}}$$

TABLE A1
Fractionation factors as function of T

Mineralogy	$10^3 \ln \alpha$	Source
Calcite, carbonate- CO_2 , acid	$\frac{3.59 \times 10^3}{T_{\text{rxn}}} - 1.79$	Kim and others, 2007
Siderite, carbonate- CO_2 , acid	$\frac{6.84 \times 10^6}{T_{\text{rxn}}^2} + 3.85$	Rosenbaum and Sheppard, 1986
Calcite, carbonate-water	$\frac{18.03 \times 10^3}{T_{\text{fm}}} - 32.42$	Kim and O'Neil, 1997
Siderite, carbonate-water	$\frac{2.56 \times 10^6}{T_{\text{fm}}^2} + 1.69$	Zhang and others, 2001

Organic Samples

Sample preparation.—The outer 1 to 2 mm of each sample was physically removed with a Dremel tool with a tungsten carbide bit and then each sample was broken into $\sim 1 \text{ cm}^3$ pieces. Any discolored fracture surfaces were further abraded with the Dremel tool. Samples were then leached with 0.1 M HCl, rinsed with de-ionized water, air-dried, soaked in dichloromethane three times for 15 minutes each and air dried again. Samples were crushed to a fine powder in a SPEX ball mill. Powdered samples were loaded into pre-extracted cellulose thimbles and the lipids were extracted with 10 percent methanol in dichloromethane (v/v) under reflux in a Soxhlet extractor for 24 hours. Elemental sulfur was removed by adding activated copper metal granules to the Soxhlet round bottom flask during the extraction. Total lipid extracts (TLE) were rotovapped to near dryness, transferred to 4 ml screwcap vials and evaporated to dryness with a gentle flow of N_2 gas.

Lipid purification.—The TLE was separated with silica gel column chromatography into an aliphatic (F1), acid (F2), and polar (F3) fractions. Soxhlet extracted silica gel was activated at 200 °C for 2 hours and 2.0 g were wet-packed into 6 ml Varian Bond-Elute SPE cartridges. The column was rinsed with ~ 3 bed volumes of hexane and the sample dissolved in hexane was loaded onto the column and eluted with 5 ml of 10 percent dichloromethane in hexane (F1), 8 ml of ethyl acetate (F2) and 5 ml of methanol (F3). The aliphatic fraction was further separated into saturated (4.5 ml hexane) and unsaturated fractions (4.5 ml ethyl acetate) with a silver-ion impregnated silica gel column (0.5 g of 5% w/w AgNO_3 silica gel) in a Pasteur pipette. Branched and cyclic compounds were removed from the saturated fraction with a zeolite molecular sieve. The sample in iso-octane was heated with 0.4 g of 5A molecular sieve at 110 °C for 12 hours. The

branched/cyclic fraction was recovered by washing the molecular sieve with hot iso-octane. The n-alkyl fraction was recovered by dissolving the molecular sieve in hydrofluoric acid and extracting the alkanes into hexane.

Molecular characterization and quantification.—Lipid fractions were characterized and quantified with an Agilent 6890 gas chromatograph equipped with a split/splitless injector, 30 meter DB-5 column (0.25 μm diameter, 0.25 μm phase thickness) coupled to an Agilent 5973 quadrupole mass spectrometer (MS) through a heated transfer line (320 °C). Samples were injected in hexane in the injector held splitless at 300 °C at a constant column helium flow of 2.0 $\text{cm}^3 \text{min}^{-1}$. The oven was held at 60 °C for 1 minute, ramped at 15 °C min^{-1} to 170 °C and 5 °C min^{-1} to 320 °C. The MS source was operated at an electron energy of 70 eV and data acquired in scan mode (50–550 m/z). Compounds were identified by elution time, comparison with published spectra (Philp, 1985; Peters and others, 2004) and authentic standards and quantified from the total ion current trace or extracted single ion traces.

Molecular hydrogen isotope analysis.—Compound specific hydrogen isotope ratios were measured using an Agilent 6890 gas chromatograph coupled to a Thermo Delta Plus XP isotope ratio monitoring mass spectrometer through a high temperature conversion reactor (Burgoyne and Hayes, 1998). Analytical conditions for the gas chromatograph were similar to those for GC-MS analysis. The high temperature reactor consisted of a 30 cm alumina tube (1/16" o.d., 0.5 mm i.d., Bolt Technical Ceramics) heated to 1430 °C and conditioned with two 1 μl injections of hexane. Every sample was co-injected with a laboratory standard containing molecules [n-C₁₄ alkane, 5 α (H)-androstane, squalane and n-C₄₁ alkane] whose δD values were determined via offline pyrolysis and dual-inlet analysis by Arndt Schimmelmann (Indiana University). The contribution of H_3^+ to the m/z 3 ion beam was subtracted using a point-wise correction (Sessions and others, 2001) in the Isodat software package. The H_3^+ factor was measured daily with increasing amplitude pulses of our H_2 laboratory reference gas. Each GC-MS analysis included pulses of laboratory H_2 reference gas at the beginning and end of the GC oven program that were used to correct for instrumental drift over the course of the run. The isotopic composition of sample molecules on the VSMOW scale was calculated from the known δD value of co-injected n-C₄₁ alkane. The long-term precision and accuracy of the system were monitored with co-injected androstane. All reported sample values had peak areas larger than a minimum threshold below which δD values vary with peak area [20 V-s for our system, Polissar and others (2009)].

APPENDIX B

TABLE B1

R₀ values and estimated burial temperatures for Oiyug Basin organic samples

Stratigraphic Unit	Sample	TAI Equivalent R ₀ Value	Estimated Burial Temperature (°C)
Oiyug Fm.	621J	0.3-0.4	23-53
	621G	0.3-0.4	23-53
	621E	0.3-0.4	23-53
	621D	0.3-0.4	23-53
	621B	0.3-0.4	23-53
	621A	0.4-0.5	53-76
	618G	0.4-0.5	53-76
U. Gazhacun Gp.	618F	0.4-0.5	53-76
	618E	0.4-0.5	53-76
	618B	0.4-0.5	53-76
	553	0.3-0.4	23-53
M. Gazhacun Gp.	551	0.4-0.5	53-76
	549	0.6-0.7	95-111
	545	0.6-0.7	95-111
L. Gazhacun Gp.	544B	0.6-0.7	95-111
	542	0.6-0.7	95-111
	577	0.6-0.7	95-111
Rigongla Fm.	575F	0.7-0.8	111-125
	575D	0.7-0.8	111-125
	572B	0.6-0.7	95-111

TABLE B3
Organic biomarker distribution and thermal maturity indices

Stratigraphic Unit	Sample Code	Lithology	Paleoenvironmental origin of identified kerogens	Average chain length ¹	OEP (C ₂₅ -C ₄₅) ²	OEP (C ₁₁ -C ₄₅) ²	20S/(20S+20R) ³
Oiyug Fm.	621J	mudstone	Fluvial/Deltaic	28.0	10.5	6.1	0.25
	621G	shale	Swamp/Deltaic	27.6	8.1	5.0	0.21
	621E	mudstone	Fluvial/Deltaic	27.8	5.7	3.7	0.19
	621D	mudstone	Fluvial/Deltaic	27.8	6.9	4.4	0.20
	621B	mudstone	Fluvial/Deltaic	28.2	6.8	4.9	0.19
	621A	mudstone	Fluvial/Deltaic	28.8	8.1	6.2	0.20
U. Gazhacun Gp.	618G	mudstone	Swamp/Deltaic	24.0	3.3	1.7	0.24
	618F	mudstone	Swamp/Deltaic	25.0	2.9	1.8	0.19
	618E	shale	Swamp/Deltaic	24.9	2.7	3.4	0.23
	618B	shale	Swamp/Deltaic	24.0	4.3	1.8	0.22

1 - Calculated from C11-45 n-alkanes.

2 - Odd over even preference.

3 - 5a,14a,17a ethylcholestane 20S/(20S+20R) calculated from m/z 217 peak areas.

TABLE B4
n-Alkane and inferred water δD values from Nanning-Oiyug samples (‰ VSMOW)

Stratigraphic Unit	Sample Code	<i>n</i> -C ₁₅	<i>n</i> -C ₁₆	<i>n</i> -C ₁₇	<i>n</i> -C ₁₈	<i>n</i> -C ₁₉	<i>n</i> -C ₂₀	<i>n</i> -C ₂₁	<i>n</i> -C ₂₂	<i>n</i> -C ₂₃	<i>n</i> -C ₂₄	<i>n</i> -C ₂₅	<i>n</i> -C ₂₆	<i>n</i> -C ₂₇	<i>n</i> -C ₂₈	<i>n</i> -C ₂₉	<i>n</i> -C ₃₀	<i>n</i> -C ₃₁	<i>n</i> -C ₃₂	<i>n</i> -C ₃₃	<i>n</i> -C ₃₄	<i>n</i> -C ₃₅	<i>n</i> -C ₃₆	<i>n</i> -C ₃₇	<i>n</i> -C ₃₈	<i>n</i> -C ₃₉	<i>n</i> -C ₄₀	<i>n</i> -C ₄₁	<i>n</i> -C ₄₂	<i>n</i> -C ₄₃	<i>n</i> -C ₄₄	<i>n</i> -C ₄₅	<i>n</i> -C ₄₆	<i>n</i> -C ₄₇	<i>n</i> -C ₄₈	<i>n</i> -C ₄₉	<i>n</i> -C ₅₀	<i>n</i> -C ₅₁	<i>n</i> -C ₅₂	<i>n</i> -C ₅₃	<i>n</i> -C ₅₄	<i>n</i> -C ₅₅	<i>n</i> -C ₅₆	<i>n</i> -C ₅₇	<i>n</i> -C ₅₈	<i>n</i> -C ₅₉	<i>n</i> -C ₆₀	<i>n</i> -C ₆₁	<i>n</i> -C ₆₂	<i>n</i> -C ₆₃	<i>n</i> -C ₆₄	<i>n</i> -C ₆₅	<i>n</i> -C ₆₆	<i>n</i> -C ₆₇	<i>n</i> -C ₆₈	<i>n</i> -C ₆₉	<i>n</i> -C ₇₀	<i>n</i> -C ₇₁	<i>n</i> -C ₇₂	<i>n</i> -C ₇₃	<i>n</i> -C ₇₄	<i>n</i> -C ₇₅	<i>n</i> -C ₇₆	<i>n</i> -C ₇₇	<i>n</i> -C ₇₈	<i>n</i> -C ₇₉	<i>n</i> -C ₈₀	<i>n</i> -C ₈₁	<i>n</i> -C ₈₂	<i>n</i> -C ₈₃	<i>n</i> -C ₈₄	<i>n</i> -C ₈₅	<i>n</i> -C ₈₆	<i>n</i> -C ₈₇	<i>n</i> -C ₈₈	<i>n</i> -C ₈₉	<i>n</i> -C ₉₀	<i>n</i> -C ₉₁	<i>n</i> -C ₉₂	<i>n</i> -C ₉₃	<i>n</i> -C ₉₄	<i>n</i> -C ₉₅	<i>n</i> -C ₉₆	<i>n</i> -C ₉₇	<i>n</i> -C ₉₈	<i>n</i> -C ₉₉	<i>n</i> -C ₁₀₀	<i>n</i> -C ₁₀₁	<i>n</i> -C ₁₀₂	<i>n</i> -C ₁₀₃	<i>n</i> -C ₁₀₄	<i>n</i> -C ₁₀₅	<i>n</i> -C ₁₀₆	<i>n</i> -C ₁₀₇	<i>n</i> -C ₁₀₈	<i>n</i> -C ₁₀₉	<i>n</i> -C ₁₁₀	<i>n</i> -C ₁₁₁	<i>n</i> -C ₁₁₂	<i>n</i> -C ₁₁₃	<i>n</i> -C ₁₁₄	<i>n</i> -C ₁₁₅	<i>n</i> -C ₁₁₆	<i>n</i> -C ₁₁₇	<i>n</i> -C ₁₁₈	<i>n</i> -C ₁₁₉	<i>n</i> -C ₁₂₀	<i>n</i> -C ₁₂₁	<i>n</i> -C ₁₂₂	<i>n</i> -C ₁₂₃	<i>n</i> -C ₁₂₄	<i>n</i> -C ₁₂₅	<i>n</i> -C ₁₂₆	<i>n</i> -C ₁₂₇	<i>n</i> -C ₁₂₈	<i>n</i> -C ₁₂₉	<i>n</i> -C ₁₃₀	<i>n</i> -C ₁₃₁	<i>n</i> -C ₁₃₂	<i>n</i> -C ₁₃₃	<i>n</i> -C ₁₃₄	<i>n</i> -C ₁₃₅	<i>n</i> -C ₁₃₆	<i>n</i> -C ₁₃₇	<i>n</i> -C ₁₃₈	<i>n</i> -C ₁₃₉	<i>n</i> -C ₁₄₀	<i>n</i> -C ₁₄₁	<i>n</i> -C ₁₄₂	<i>n</i> -C ₁₄₃	<i>n</i> -C ₁₄₄	<i>n</i> -C ₁₄₅	<i>n</i> -C ₁₄₆	<i>n</i> -C ₁₄₇	<i>n</i> -C ₁₄₈	<i>n</i> -C ₁₄₉	<i>n</i> -C ₁₅₀	<i>n</i> -C ₁₅₁	<i>n</i> -C ₁₅₂	<i>n</i> -C ₁₅₃	<i>n</i> -C ₁₅₄	<i>n</i> -C ₁₅₅	<i>n</i> -C ₁₅₆	<i>n</i> -C ₁₅₇	<i>n</i> -C ₁₅₈	<i>n</i> -C ₁₅₉	<i>n</i> -C ₁₆₀	<i>n</i> -C ₁₆₁	<i>n</i> -C ₁₆₂	<i>n</i> -C ₁₆₃	<i>n</i> -C ₁₆₄	<i>n</i> -C ₁₆₅	<i>n</i> -C ₁₆₆	<i>n</i> -C ₁₆₇	<i>n</i> -C ₁₆₈	<i>n</i> -C ₁₆₉	<i>n</i> -C ₁₇₀	<i>n</i> -C ₁₇₁	<i>n</i> -C ₁₇₂	<i>n</i> -C ₁₇₃	<i>n</i> -C ₁₇₄	<i>n</i> -C ₁₇₅	<i>n</i> -C ₁₇₆	<i>n</i> -C ₁₇₇	<i>n</i> -C ₁₇₈	<i>n</i> -C ₁₇₉	<i>n</i> -C ₁₈₀	<i>n</i> -C ₁₈₁	<i>n</i> -C ₁₈₂	<i>n</i> -C ₁₈₃	<i>n</i> -C ₁₈₄	<i>n</i> -C ₁₈₅	<i>n</i> -C ₁₈₆	<i>n</i> -C ₁₈₇	<i>n</i> -C ₁₈₈	<i>n</i> -C ₁₈₉	<i>n</i> -C ₁₉₀	<i>n</i> -C ₁₉₁	<i>n</i> -C ₁₉₂	<i>n</i> -C ₁₉₃	<i>n</i> -C ₁₉₄	<i>n</i> -C ₁₉₅	<i>n</i> -C ₁₉₆	<i>n</i> -C ₁₉₇	<i>n</i> -C ₁₉₈	<i>n</i> -C ₁₉₉	<i>n</i> -C ₂₀₀	<i>n</i> -C ₂₀₁	<i>n</i> -C ₂₀₂	<i>n</i> -C ₂₀₃	<i>n</i> -C ₂₀₄	<i>n</i> -C ₂₀₅	<i>n</i> -C ₂₀₆	<i>n</i> -C ₂₀₇	<i>n</i> -C ₂₀₈	<i>n</i> -C ₂₀₉	<i>n</i> -C ₂₁₀	<i>n</i> -C ₂₁₁	<i>n</i> -C ₂₁₂	<i>n</i> -C ₂₁₃	<i>n</i> -C ₂₁₄	<i>n</i> -C ₂₁₅	<i>n</i> -C ₂₁₆	<i>n</i> -C ₂₁₇	<i>n</i> -C ₂₁₈	<i>n</i> -C ₂₁₉	<i>n</i> -C ₂₂₀	<i>n</i> -C ₂₂₁	<i>n</i> -C ₂₂₂	<i>n</i> -C ₂₂₃	<i>n</i> -C ₂₂₄	<i>n</i> -C ₂₂₅	<i>n</i> -C ₂₂₆	<i>n</i> -C ₂₂₇	<i>n</i> -C ₂₂₈	<i>n</i> -C ₂₂₉	<i>n</i> -C ₂₃₀	<i>n</i> -C ₂₃₁	<i>n</i> -C ₂₃₂	<i>n</i> -C ₂₃₃	<i>n</i> -C ₂₃₄	<i>n</i> -C ₂₃₅	<i>n</i> -C ₂₃₆	<i>n</i> -C ₂₃₇	<i>n</i> -C ₂₃₈	<i>n</i> -C ₂₃₉	<i>n</i> -C ₂₄₀	<i>n</i> -C ₂₄₁	<i>n</i> -C ₂₄₂	<i>n</i> -C ₂₄₃	<i>n</i> -C ₂₄₄	<i>n</i> -C ₂₄₅	<i>n</i> -C ₂₄₆	<i>n</i> -C ₂₄₇	<i>n</i> -C ₂₄₈	<i>n</i> -C ₂₄₉	<i>n</i> -C ₂₅₀	<i>n</i> -C ₂₅₁	<i>n</i> -C ₂₅₂	<i>n</i> -C ₂₅₃	<i>n</i> -C ₂₅₄	<i>n</i> -C ₂₅₅	<i>n</i> -C ₂₅₆	<i>n</i> -C ₂₅₇	<i>n</i> -C ₂₅₈	<i>n</i> -C ₂₅₉	<i>n</i> -C ₂₆₀	<i>n</i> -C ₂₆₁	<i>n</i> -C ₂₆₂	<i>n</i> -C ₂₆₃	<i>n</i> -C ₂₆₄	<i>n</i> -C ₂₆₅	<i>n</i> -C ₂₆₆	<i>n</i> -C ₂₆₇	<i>n</i> -C ₂₆₈	<i>n</i> -C ₂₆₉	<i>n</i> -C ₂₇₀	<i>n</i> -C ₂₇₁	<i>n</i> -C ₂₇₂	<i>n</i> -C ₂₇₃	<i>n</i> -C ₂₇₄	<i>n</i> -C ₂₇₅	<i>n</i> -C ₂₇₆	<i>n</i> -C ₂₇₇	<i>n</i> -C ₂₇₈	<i>n</i> -C ₂₇₉	<i>n</i> -C ₂₈₀	<i>n</i> -C ₂₈₁	<i>n</i> -C ₂₈₂	<i>n</i> -C ₂₈₃	<i>n</i> -C ₂₈₄	<i>n</i> -C ₂₈₅	<i>n</i> -C ₂₈₆	<i>n</i> -C ₂₈₇	<i>n</i> -C ₂₈₈	<i>n</i> -C ₂₈₉	<i>n</i> -C ₂₉₀	<i>n</i> -C ₂₉₁	<i>n</i> -C ₂₉₂	<i>n</i> -C ₂₉₃	<i>n</i> -C ₂₉₄	<i>n</i> -C ₂₉₅	<i>n</i> -C ₂₉₆	<i>n</i> -C ₂₉₇	<i>n</i> -C ₂₉₈	<i>n</i> -C ₂₉₉	<i>n</i> -C ₃₀₀	<i>n</i> -C ₃₀₁	<i>n</i> -C ₃₀₂	<i>n</i> -C ₃₀₃	<i>n</i> -C ₃₀₄	<i>n</i> -C ₃₀₅	<i>n</i> -C ₃₀₆	<i>n</i> -C ₃₀₇	<i>n</i> -C ₃₀₈	<i>n</i> -C ₃₀₉	<i>n</i> -C ₃₁₀	<i>n</i> -C ₃₁₁	<i>n</i> -C ₃₁₂	<i>n</i> -C ₃₁₃	<i>n</i> -C ₃₁₄	<i>n</i> -C ₃₁₅	<i>n</i> -C ₃₁₆	<i>n</i> -C ₃₁₇	<i>n</i> -C ₃₁₈	<i>n</i> -C ₃₁₉	<i>n</i> -C ₃₂₀	<i>n</i> -C ₃₂₁	<i>n</i> -C ₃₂₂	<i>n</i> -C ₃₂₃	<i>n</i> -C ₃₂₄	<i>n</i> -C ₃₂₅	<i>n</i> -C ₃₂₆	<i>n</i> -C ₃₂₇	<i>n</i> -C ₃₂₈	<i>n</i> -C ₃₂₉	<i>n</i> -C ₃₃₀	<i>n</i> -C ₃₃₁	<i>n</i> -C ₃₃₂	<i>n</i> -C ₃₃₃	<i>n</i> -C ₃₃₄	<i>n</i> -C ₃₃₅	<i>n</i> -C ₃₃₆	<i>n</i> -C ₃₃₇	<i>n</i> -C ₃₃₈	<i>n</i> -C ₃₃₉	<i>n</i> -C ₃₄₀	<i>n</i> -C ₃₄₁	<i>n</i> -C ₃₄₂	<i>n</i> -C ₃₄₃	<i>n</i> -C ₃₄₄	<i>n</i> -C ₃₄₅	<i>n</i> -C ₃₄₆	<i>n</i> -C ₃₄₇	<i>n</i> -C ₃₄₈	<i>n</i> -C ₃₄₉	<i>n</i> -C ₃₅₀	<i>n</i> -C ₃₅₁	<i>n</i> -C ₃₅₂	<i>n</i> -C ₃₅₃	<i>n</i> -C ₃₅₄	<i>n</i> -C ₃₅₅	<i>n</i> -C ₃₅₆	<i>n</i> -C ₃₅₇	<i>n</i> -C ₃₅₈	<i>n</i> -C ₃₅₉	<i>n</i> -C ₃₆₀	<i>n</i> -C ₃₆₁	<i>n</i> -C ₃₆₂	<i>n</i> -C ₃₆₃	<i>n</i> -C ₃₆₄	<i>n</i> -C ₃₆₅	<i>n</i> -C ₃₆₆	<i>n</i> -C ₃₆₇	<i>n</i> -C ₃₆₈	<i>n</i> -C ₃₆₉	<i>n</i> -C ₃₇₀	<i>n</i> -C ₃₇₁	<i>n</i> -C ₃₇₂	<i>n</i> -C ₃₇₃	<i>n</i> -C ₃₇₄	<i>n</i> -C ₃₇₅	<i>n</i> -C ₃₇₆	<i>n</i> -C ₃₇₇	<i>n</i> -C ₃₇₈	<i>n</i> -C ₃₇₉	<i>n</i> -C ₃₈₀	<i>n</i> -C ₃₈₁	<i>n</i> -C ₃₈₂	<i>n</i> -C ₃₈₃	<i>n</i> -C ₃₈₄	<i>n</i> -C ₃₈₅	<i>n</i> -C ₃₈₆	<i>n</i> -C ₃₈₇	<i>n</i> -C ₃₈₈	<i>n</i> -C ₃₈₉	<i>n</i> -C ₃₉₀	<i>n</i> -C ₃₉₁	<i>n</i> -C ₃₉₂	<i>n</i> -C ₃₉₃	<i>n</i> -C ₃₉₄	<i>n</i> -C ₃₉₅	<i>n</i> -C ₃₉₆	<i>n</i> -C ₃₉₇	<i>n</i> -C ₃₉₈	<i>n</i> -C ₃₉₉	<i>n</i> -C ₄₀₀	<i>n</i> -C ₄₀₁	<i>n</i> -C ₄₀₂	<i>n</i> -C ₄₀₃	<i>n</i> -C ₄₀₄	<i>n</i> -C ₄₀₅	<i>n</i> -C ₄₀₆	<i>n</i> -C ₄₀₇	<i>n</i> -C ₄₀₈	<i>n</i> -C ₄₀₉	<i>n</i> -C ₄₁₀	<i>n</i> -C ₄₁₁	<i>n</i> -C ₄₁₂	<i>n</i> -C ₄₁₃	<i>n</i> -C ₄₁₄	<i>n</i> -C ₄₁₅	<i>n</i> -C ₄₁₆	<i>n</i> -C ₄₁₇	<i>n</i> -C ₄₁₈	<i>n</i> -C ₄₁₉	<i>n</i> -C ₄₂₀	<i>n</i> -C ₄₂₁	<i>n</i> -C ₄₂₂	<i>n</i> -C ₄₂₃	<i>n</i> -C ₄₂₄	<i>n</i> -C ₄₂₅	<i>n</i> -C ₄₂₆	<i>n</i> -C ₄₂₇	<i>n</i> -C ₄₂₈	<i>n</i> -C ₄₂₉	<i>n</i> -C ₄₃₀	<i>n</i> -C ₄₃₁	<i>n</i> -C ₄₃₂	<i>n</i> -C ₄₃₃	<i>n</i> -C ₄₃₄	<i>n</i> -C ₄₃₅	<i>n</i> -C ₄₃₆	<i>n</i> -C ₄₃₇	<i>n</i> -C ₄₃₈	<i>n</i> -C ₄₃₉	<i>n</i> -C ₄₄₀	<i>n</i> -C ₄₄₁	<i>n</i> -C ₄₄₂	<i>n</i> -C ₄₄₃	<i>n</i> -C ₄₄₄	<i>n</i> -C ₄₄₅	<i>n</i> -C ₄₄₆	<i>n</i> -C ₄₄₇	<i>n</i> -C ₄₄₈	<i>n</i> -C ₄₄₉	<i>n</i> -C ₄₅₀	<i>n</i> -C ₄₅₁	<i>n</i> -C ₄₅₂	<i>n</i> -C ₄₅₃	<i>n</i> -C ₄₅₄	<i>n</i> -C ₄₅₅	<i>n</i> -C ₄₅₆	<i>n</i> -C ₄₅₇	<i>n</i> -C ₄₅₈	<i>n</i> -C ₄₅₉	<i>n</i> -C ₄₆₀	<i>n</i> -C ₄₆₁	<i>n</i> -C ₄₆₂	<i>n</i> -C ₄₆₃	<i>n</i> -C ₄₆₄	<i>n</i> -C ₄₆₅	<i>n</i> -C ₄₆₆	<i>n</i> -C ₄₆₇	<i>n</i> -C ₄₆₈	<i>n</i> -C ₄₆₉	<i>n</i> -C ₄₇₀	<i>n</i> -C ₄₇₁	<i>n</i> -C ₄₇₂	<i>n</i> -C ₄₇₃	<i>n</i> -C ₄₇₄	<i>n</i> -C ₄₇₅	<i>n</i> -C ₄₇₆	<i>n</i> -C ₄₇₇	<i>n</i> -C ₄₇₈	<i>n</i> -C ₄₇₉	<i>n</i> -C ₄₈₀	<i>n</i> -C ₄₈₁	<i>n</i> -C ₄₈₂	<i>n</i> -C ₄₈₃	<i>n</i> -C ₄₈₄	<i>n</i> -C ₄₈₅	<i>n</i> -C ₄₈₆	<i>n</i> -C ₄₈₇	<i>n</i> -C ₄₈₈	<i>n</i> -C ₄₈₉	<i>n</i> -C ₄₉₀	<i>n</i> -C ₄₉₁	<i>n</i> -C ₄₉₂	<i>n</i> -C ₄₉₃	<i>n</i> -C ₄₉₄	<i>n</i> -C ₄₉₅	<i>n</i> -C ₄₉₆	<i>n</i> -C ₄₉₇	<i>n</i> -C ₄₉₈	<i>n</i> -C ₄₉₉	<i>n</i> -C ₅₀₀	<i>n</i> -C ₅₀₁	<i>n</i> -C ₅₀₂	<i>n</i> -C ₅₀₃	<i>n</i> -C ₅₀₄	<i>n</i> -C ₅₀₅	<i>n</i> -C ₅₀₆	<i>n</i> -C ₅₀₇	<i>n</i> -C ₅₀₈	<i>n</i> -C ₅₀₉	<i>n</i> -C ₅₁₀	<i>n</i> -C ₅₁₁	<i>n</i> -C ₅₁₂	<i>n</i> -C ₅₁₃	<i>n</i> -C ₅₁₄	<i>n</i> -C ₅₁₅	<i>n</i> -C ₅₁₆	<i>n</i> -C ₅₁₇	<i>n</i> -C ₅₁₈	<i>n</i> -C ₅₁₉	<i>n</i> -C ₅₂₀	<i>n</i> -C ₅₂₁	<i>n</i> -C ₅₂₂	<i>n</i> -C ₅₂₃	<i>n</i> -C ₅₂₄	<i>n</i> -C ₅₂₅	<i>n</i> -C ₅₂₆	<i>n</i> -C ₅₂₇	<i>n</i> -C ₅₂₈	<i>n</i> -C ₅₂₉	<i>n</i> -C ₅₃₀	<i>n</i> -C ₅₃₁	<i>n</i> -C ₅₃₂	<i>n</i> -C ₅₃₃	<i>n</i> -C ₅₃₄	<i>n</i> -C ₅₃₅	<i>n</i> -C ₅₃₆	<i>n</i> -C ₅₃₇	<i>n</i> -C ₅₃₈	<i>n</i> -C ₅₃₉	<i>n</i> -C ₅₄₀	<i>n</i> -C ₅₄₁	<i>n</i> -C ₅₄₂	<i>n</i> -C ₅₄₃	<i>n</i> -C ₅₄₄	<i>n</i> -C ₅₄₅	<i>n</i> -C ₅₄₆	<i>n</i> -C ₅₄₇	<i>n</i> -C ₅₄₈	<i>n</i> -C ₅₄₉	<i>n</i> -C ₅₅₀	<i>n</i> -C ₅₅₁	<i>n</i> -C ₅₅₂	<i>n</i> -C ₅₅₃	<i>n</i> -C ₅₅₄	<i>n</i> -C ₅₅₅	<i>n</i> -C ₅₅₆	<i>n</i> -C ₅₅₇	<i>n</i> -C ₅₅₈	<i>n</i> -C ₅₅₉	<i>n</i> -C ₅₆₀	<i>n</i> -C ₅₆₁	<i>n</i> -C ₅₆₂	<i>n</i> -C ₅₆₃	<i>n</i> -C ₅₆₄	<i>n</i> -C ₅₆₅	<i>n</i> -C ₅₆₆	<i>n</i> -C ₅₆₇	<i>n</i> -C ₅₆₈	<i>n</i> -C ₅₆₉	<i>n</i> -C ₅₇₀	<i>n</i> -C ₅₇₁	<i>n</i> -C ₅₇₂	<i>n</i> -C ₅₇₃	<i>n</i> -C ₅₇₄	<i>n</i> -C ₅₇₅	<i>n</i> -C ₅₇₆	<i>n</i> -C ₅₇₇	<i>n</i> -C ₅₇₈	<i>n</i> -C ₅₇₉	<i>n</i> -C ₅₈₀	<i>n</i> -C ₅₈₁	<i>n</i> -C ₅₈₂	<i>n</i> -C ₅₈₃	<i>n</i> -C ₅₈₄	<i>n</i> -C ₅₈₅	<i>n</i> -C ₅₈₆	<i>n</i> -C ₅₈₇	<i>n</i> -C ₅₈₈	<i>n</i> -C ₅₈₉	<i>n</i> -C ₅₉₀	<i>n</i> -C ₅₉₁	<i>n</i> -C ₅₉₂	<i>n</i> -C ₅₉₃	<i>n</i> -C ₅₉₄	<i>n</i> -C ₅₉₅	<i>n</i> -C ₅₉₆	<i>n</i> -C ₅₉₇	<i>n</i> -C ₅₉₈	<i>n</i> -C ₅₉₉	<i>n</i> -C ₆₀₀	<i>n</i> -C ₆₀₁	<i>n</i> -C ₆₀₂	<i>n</i> -C ₆₀₃	<i>n</i> -C ₆₀₄	<i>n</i> -C ₆₀₅	<i>n</i> -C ₆₀₆	<i>n</i> -C ₆₀₇	<i>n</i> -C ₆₀₈	<i>n</i> -C ₆₀₉	<i>n</i> -C ₆₁₀	<i>n</i> -C ₆₁₁	<i>n</i> -C ₆₁₂	<i>n</i> -C ₆₁₃	<i>n</i> -C ₆₁₄	<i>n</i> -C ₆₁₅	<i>n</i> -C ₆₁₆	<i>n</i> -C ₆₁₇	<i>n</i> -C ₆₁₈	<i>n</i> -C ₆₁₉	<i>n</i> -C ₆₂₀	<i>n</i> -C ₆₂₁	<i>n</i> -C ₆₂₂	<i>n</i> -C ₆₂₃	<i>n</i> -C ₆₂₄	<i>n</i> -C ₆₂₅	<i>n</i> -C ₆₂₆	<i>n</i> -C ₆₂₇	<i>n</i> -C ₆₂
--------------------	-------------	---------------------------	---------------------------	---------------------------	---------------------------	---------------------------	---------------------------	---------------------------	---------------------------	---------------------------	---------------------------	---------------------------	---------------------------	---------------------------	---------------------------	---------------------------	---------------------------	---------------------------	---------------------------	---------------------------	---------------------------	---------------------------	---------------------------	---------------------------	---------------------------	---------------------------	---------------------------	---------------------------	---------------------------	---------------------------	---------------------------	---------------------------	---------------------------	---------------------------	---------------------------	---------------------------	---------------------------	---------------------------	---------------------------	---------------------------	---------------------------	---------------------------	---------------------------	---------------------------	---------------------------	---------------------------	---------------------------	---------------------------	---------------------------	---------------------------	---------------------------	---------------------------	---------------------------	---------------------------	---------------------------	---------------------------	---------------------------	---------------------------	---------------------------	---------------------------	---------------------------	---------------------------	---------------------------	---------------------------	---------------------------	---------------------------	---------------------------	---------------------------	---------------------------	---------------------------	---------------------------	---------------------------	---------------------------	---------------------------	---------------------------	---------------------------	---------------------------	---------------------------	---------------------------	---------------------------	---------------------------	---------------------------	---------------------------	---------------------------	---------------------------	---------------------------	----------------------------	----------------------------	----------------------------	----------------------------	----------------------------	----------------------------	----------------------------	----------------------------	----------------------------	----------------------------	----------------------------	----------------------------	----------------------------	----------------------------	----------------------------	----------------------------	----------------------------	----------------------------	----------------------------	----------------------------	----------------------------	----------------------------	----------------------------	----------------------------	----------------------------	----------------------------	----------------------------	----------------------------	----------------------------	----------------------------	----------------------------	----------------------------	----------------------------	----------------------------	----------------------------	----------------------------	----------------------------	----------------------------	----------------------------	----------------------------	----------------------------	----------------------------	----------------------------	----------------------------	----------------------------	----------------------------	----------------------------	----------------------------	----------------------------	----------------------------	----------------------------	----------------------------	----------------------------	----------------------------	----------------------------	----------------------------	----------------------------	----------------------------	----------------------------	----------------------------	----------------------------	----------------------------	----------------------------	----------------------------	----------------------------	----------------------------	----------------------------	----------------------------	----------------------------	----------------------------	----------------------------	----------------------------	----------------------------	----------------------------	----------------------------	----------------------------	----------------------------	----------------------------	----------------------------	----------------------------	----------------------------	----------------------------	----------------------------	----------------------------	----------------------------	----------------------------	----------------------------	----------------------------	----------------------------	----------------------------	----------------------------	----------------------------	----------------------------	----------------------------	----------------------------	----------------------------	----------------------------	----------------------------	----------------------------	----------------------------	----------------------------	----------------------------	----------------------------	----------------------------	----------------------------	----------------------------	----------------------------	----------------------------	----------------------------	----------------------------	----------------------------	----------------------------	----------------------------	----------------------------	----------------------------	----------------------------	----------------------------	----------------------------	----------------------------	----------------------------	----------------------------	----------------------------	----------------------------	----------------------------	----------------------------	----------------------------	----------------------------	----------------------------	----------------------------	----------------------------	----------------------------	----------------------------	----------------------------	----------------------------	----------------------------	----------------------------	----------------------------	----------------------------	----------------------------	----------------------------	----------------------------	----------------------------	----------------------------	----------------------------	----------------------------	----------------------------	----------------------------	----------------------------	----------------------------	----------------------------	----------------------------	----------------------------	----------------------------	----------------------------	----------------------------	----------------------------	----------------------------	----------------------------	----------------------------	----------------------------	----------------------------	----------------------------	----------------------------	----------------------------	----------------------------	----------------------------	----------------------------	----------------------------	----------------------------	----------------------------	----------------------------	----------------------------	----------------------------	----------------------------	----------------------------	----------------------------	----------------------------	----------------------------	----------------------------	----------------------------	----------------------------	----------------------------	----------------------------	----------------------------	----------------------------	----------------------------	----------------------------	----------------------------	----------------------------	----------------------------	----------------------------	----------------------------	----------------------------	----------------------------	----------------------------	----------------------------	----------------------------	----------------------------	----------------------------	----------------------------	----------------------------	----------------------------	----------------------------	----------------------------	----------------------------	----------------------------	----------------------------	----------------------------	----------------------------	----------------------------	----------------------------	----------------------------	----------------------------	----------------------------	----------------------------	----------------------------	----------------------------	----------------------------	----------------------------	----------------------------	----------------------------	----------------------------	----------------------------	----------------------------	----------------------------	----------------------------	----------------------------	----------------------------	----------------------------	----------------------------	----------------------------	----------------------------	----------------------------	----------------------------	----------------------------	----------------------------	----------------------------	----------------------------	----------------------------	----------------------------	----------------------------	----------------------------	----------------------------	----------------------------	----------------------------	----------------------------	----------------------------	----------------------------	----------------------------	----------------------------	----------------------------	----------------------------	----------------------------	----------------------------	----------------------------	----------------------------	----------------------------	----------------------------	----------------------------	----------------------------	----------------------------	----------------------------	----------------------------	----------------------------	----------------------------	----------------------------	----------------------------	----------------------------	----------------------------	----------------------------	----------------------------	----------------------------	----------------------------	----------------------------	----------------------------	----------------------------	----------------------------	----------------------------	----------------------------	----------------------------	----------------------------	----------------------------	----------------------------	----------------------------	----------------------------	----------------------------	----------------------------	----------------------------	----------------------------	----------------------------	----------------------------	----------------------------	----------------------------	----------------------------	----------------------------	----------------------------	----------------------------	----------------------------	----------------------------	----------------------------	----------------------------	----------------------------	----------------------------	----------------------------	----------------------------	----------------------------	----------------------------	----------------------------	----------------------------	----------------------------	----------------------------	----------------------------	----------------------------	----------------------------	----------------------------	----------------------------	----------------------------	----------------------------	----------------------------	----------------------------	----------------------------	----------------------------	----------------------------	----------------------------	----------------------------	----------------------------	----------------------------	----------------------------	----------------------------	----------------------------	----------------------------	----------------------------	----------------------------	----------------------------	----------------------------	----------------------------	----------------------------	----------------------------	----------------------------	----------------------------	----------------------------	----------------------------	----------------------------	----------------------------	----------------------------	----------------------------	----------------------------	----------------------------	----------------------------	----------------------------	----------------------------	----------------------------	----------------------------	----------------------------	----------------------------	----------------------------	----------------------------	----------------------------	----------------------------	----------------------------	----------------------------	----------------------------	----------------------------	----------------------------	----------------------------	----------------------------	----------------------------	----------------------------	----------------------------	----------------------------	----------------------------	----------------------------	----------------------------	----------------------------	----------------------------	----------------------------	----------------------------	----------------------------	----------------------------	----------------------------	----------------------------	----------------------------	----------------------------	----------------------------	----------------------------	----------------------------	----------------------------	----------------------------	----------------------------	----------------------------	----------------------------	----------------------------	----------------------------	----------------------------	----------------------------	----------------------------	----------------------------	----------------------------	----------------------------	----------------------------	----------------------------	----------------------------	----------------------------	----------------------------	----------------------------	----------------------------	----------------------------	----------------------------	----------------------------	----------------------------	----------------------------	----------------------------	----------------------------	----------------------------	----------------------------	----------------------------	----------------------------	----------------------------	----------------------------	----------------------------	----------------------------	----------------------------	----------------------------	----------------------------	----------------------------	----------------------------	----------------------------	----------------------------	----------------------------	----------------------------	----------------------------	----------------------------	----------------------------	----------------------------	----------------------------	----------------------------	----------------------------	----------------------------	----------------------------	----------------------------	----------------------------	----------------------------	----------------------------	----------------------------	----------------------------	----------------------------	----------------------------	----------------------------	----------------------------	----------------------------	----------------------------	----------------------------	----------------------------	----------------------------	----------------------------	----------------------------	----------------------------	----------------------------	----------------------------	----------------------------	----------------------------	----------------------------	----------------------------	----------------------------	----------------------------	----------------------------	----------------------------	----------------------------	----------------------------	----------------------------	----------------------------	----------------------------	----------------------------	----------------------------	----------------------------	----------------------------	----------------------------	----------------------------	----------------------------	----------------------------	----------------------------	----------------------------	----------------------------	----------------------------	----------------------------	----------------------------	----------------------------	----------------------------	----------------------------	----------------------------	----------------------------	----------------------------	----------------------------	----------------------------	----------------------------	----------------------------	----------------------------	----------------------------	----------------------------	----------------------------	----------------------------	----------------------------	----------------------------	----------------------------	----------------------------	----------------------------	----------------------------	----------------------------	----------------------------	----------------------------	----------------------------	----------------------------	----------------------------	----------------------------	----------------------------	----------------------------	----------------------------	----------------------------	----------------------------	----------------------------	----------------------------	----------------------------	----------------------------	----------------------------	----------------------------	----------------------------	----------------------------	----------------------------	---------------------------

REFERENCES

- Barker, C. E., 1988, Geothermics of petroleum systems: Implications of the stabilization of kerogen thermal maturation after a geologically brief heating duration at peak temperature, *in* Magoon, L. B., editor, Petroleum systems of the United States: United States Geological Survey Bulletin 1870, p. 26–29.
- Bera, M. K., Sarkar, A., Tandon, S. K., Samanta, A., and Sanyal, P., 2010, Does burial diagenesis reset pristine isotopic compositions in paleosol carbonates?: Earth and Planetary Science Letters, v. 300, n. 1–2, p. 85–100, <http://dx.doi.org/10.1016/j.epsl.2010.09.040>
- Billups, K., and Schrag, D. P., 2003, Application of benthic foraminiferal Mg/Ca ratios to questions of Cenozoic climate change: Earth and Planetary Science Letters, v. 209, n. 1–2, p. 181–195, [http://dx.doi.org/10.1016/S0012-821X\(03\)00067-0](http://dx.doi.org/10.1016/S0012-821X(03)00067-0)
- Burgoyne, T. W., and Hayes, J. M., 1998, Quantitative production of H₂ by pyrolysis of gas chromatographic effluents: Analytical Chemistry, v. 70, n. 24, p. 5136–5141, <http://dx.doi.org/10.1021/ac980248v>
- Bush, R. T., and McInerney, F. A., 2013, Leaf wax *n*-alkane distributions in and across modern plants: Implications for paleoecology and chemotaxonomy: Geochimica et Cosmochimica Acta, v. 117, p. 161–179, <http://dx.doi.org/10.1016/j.gca.2013.04.016>
- Cassel, E. J., Graham, S. A., and Chamberlain, C. P., 2009, Cenozoic tectonic and topographic evolution of the northern Sierra Nevada, California, through stable isotope paleoaltimetry in volcanic glass: Geology, v. 37, n. 6, p. 547–550, <http://dx.doi.org/10.1130/G25572A.1>
- Chen, H., Han, J., Ding, Z., Sun H., and Guo, Z., 2008, Chronological dating and tectonic implications of late Cenozoic volcanic rocks and lacustrine sequence in Oiyug Basin of southern Tibet: Science in China Series D: Earth Sciences, v. 51, n. 2, p. 275–283, <http://dx.doi.org/10.1007/s11430-008-0007-6>
- Chikaraishi, Y., Suzuki, Y., and Naraoka, H., 2004, Hydrogen isotope fractionations during desaturation and elongation associated with polyunsaturated fatty acid biosynthesis in marine macroalgae: Phytochemistry, v. 65, n. 15, p. 2293–2300, <http://dx.doi.org/10.1016/j.phytochem.2004.06.030>
- Currie, B. S., Rowley, D. B., and Tabor, N. J., 2005, Middle Miocene paleoaltimetry of southern Tibet: Implications for the role of mantle thickening and delamination in the Himalayan Orogen: Geology, v. 33, n. 3, p. 181–184, <http://dx.doi.org/10.1130/G21170.1>
- Curtis, C. D., Pearson, M. J., and Somogyi, V. A., 1975, Mineralogy, chemistry, and origin of a concretionary siderite sheet (clay-ironstone band) in the Westphalian of Yorkshire: Mineralogical Magazine v. 40, p. 385–393, <http://dx.doi.org/10.1180/minmag.1975.040.312.07>
- DeCelles, P. G., Quade, J., Kapp, P., Fan, M., Dettman, D. L., and Ding, L., 2007, High and dry in central Tibet during the late Oligocene: Earth and Planetary Science Letters, v. 253, n. 3–4, p. 389–401, <http://dx.doi.org/10.1016/j.epsl.2006.11.001>
- Diefendorf, A. F., Freeman, K. H., Wing, S. L., and Graham, H. V., 2011, Production of *n*-alkyl lipids in living plants and implications for the geologic past: Geochimica et Cosmochimica Acta, v. 75, n. 23, p. 7472–7485, <http://dx.doi.org/10.1016/j.gca.2011.09.028>
- Ding, L., Xu, Q., Yue, Y., Wang, H., Cai, F., and Li, S., 2014, The Andean-type Gangdese Mountains: Paleoelevation record from the Paleocene–Eocene Linzhou Basin: Earth and Planetary Science Letters, v. 392, p. 250–264, <http://dx.doi.org/10.1016/j.epsl.2014.01.045>
- dos Santos Neto, E. V., and Hayes, J. M., 1999, Use of hydrogen and carbon stable isotopes characterizing oils from the Potiguar Basin (onshore), northeastern Brazil: American Association of Petroleum Geologists Bulletin, v. 83, n. 3, p. 496–518.
- Drummond, C. N., Patterson, W. P., and Walker, J. C. G., 1995, Climatic forcing of carbon-oxygen isotopic covariance in temperate-region marl lakes: Geology, v. 23, n. 11, p. 1031–1034, [http://dx.doi.org/10.1130/0091-7613\(1995\)023<1031:CFOCO1>2.3.CO;2](http://dx.doi.org/10.1130/0091-7613(1995)023<1031:CFOCO1>2.3.CO;2)
- France-Lanord, C., Sheppard, S. M. F., and Le Fort, P., 1988, Hydrogen and oxygen variations in the high Himalaya peraluminous Manaslu leucogranite: Evidence for heterogeneous sedimentary source: Geochimica et Cosmochimica Acta, v. 52, n. 2, p. 513–526, [http://dx.doi.org/10.1016/0016-7037\(88\)90107-X](http://dx.doi.org/10.1016/0016-7037(88)90107-X)
- Garzione, C. N., Quade, J., DeCelles, P. G., and English, N. B., 2000, Predicting paleoelevation of Tibet and the Himalaya from delta O-18 versus altitude gradients in meteoric water across the Nepal Himalaya: Earth and Planetary Science Letters, v. 183, n. 1–2, p. 215, [http://dx.doi.org/10.1016/S0012-821X\(00\)00252-1](http://dx.doi.org/10.1016/S0012-821X(00)00252-1)
- Garzione, C. N., Dettman, D. L., and Horton, B. K., 2004, Carbonate oxygen isotope paleoaltimetry: Evaluating the effect of diagenesis on paleoelevation estimates for the Tibetan plateau: Palaeogeography, Palaeoclimatology, Palaeoecology, v. 212, n. 1–2, p. 119–140, [http://dx.doi.org/10.1016/S0031-0182\(04\)00307-4](http://dx.doi.org/10.1016/S0031-0182(04)00307-4)
- Gébelin, A., Mulch, A., Teyssier, C., Jessup, M. J., Law, R. D., and Brunel, M., 2013, The Miocene elevation of Mount Everest: Geology, v. 41, n. 7, p. 799–802, <http://dx.doi.org/10.1130/G34331.1>
- Ghosh, P., Adkins, J., Affek, H., Balta, B., Guo, W. F., Schauble, E. A., Schrag, D., and Eiler, J. M., 2006, ¹³C-¹⁸O bonds in carbonate minerals: A new kind of paleothermometer: Geochimica et Cosmochimica Acta, v. 70, n. 6, p. 1439–1456, <http://dx.doi.org/10.1016/j.gca.2005.11.014>
- Gonfiantini, R., Roche, M. A., Olivry, J.-C., Fontes, J.-C., and Zuppi, G. M., 2001, The altitude effect on the isotopic composition of tropical rains: Chemical Geology, v. 181, n. 1–4, p. 147–167, [http://dx.doi.org/10.1016/S0009-2541\(01\)00279-0](http://dx.doi.org/10.1016/S0009-2541(01)00279-0)
- Gourbet, L., Maheo, G., Leloup, P. H., Jean-Louis, P., Sorrel, P., Eymard, I., Antoine, P.-O., Sterb, M., Wang, G., Cao, K., Chevalier, M.-L., and Lu, H., 2015, The Jianchuan Basin, Yunnan: Implications on the evolution of SE Tibet during the Eocene: Proceedings of the 2015 American Geophysical Union Fall Meeting, San Francisco, CA, USA, p. T12B-08.
- Harrison, T. M., Copeland, P., Kidd, W. S. F., and Lovera, O. M., 1995, Activation of the Nyainqentanglha shear zone: Implications for uplift of the southern Tibetan Plateau: Tectonics, v. 14, n. 3, p. 658–676, <http://dx.doi.org/10.1029/95TC00608>

- Heath, R. C., 1983, Basic ground-water hydrology: United States Geological Survey Water Supply Paper 2220, 86 p.
- Hoke, G. D., Jing, L. Z., Hren, M. T., Wissink, G. K., and Garziona, C. N., 2014, Stable isotopes reveal high southeast Tibetan Plateau margin since the Paleogene: *Earth and Planetary Science Letters*, v. 394, p. 270–278, <http://dx.doi.org/10.1016/j.epsl.2014.03.007>
- Horton, T. W., Sjostrom, D. J., Abruzzese, M. J., Poage, M. A., Waldbauer, J. R., Hren, M., Wooden, J., and Chamberlain, C. P., 2004, Spatial and temporal variation of Cenozoic surface elevation in the Great Basin and Sierra Nevada: *American Journal of Science*, v. 304, n. 10, p. 862–888, <http://dx.doi.org/10.2475/ajs.304.10.862>
- Hren, M. T., and Sheldon, N. D., 2012, Temporal variations in lake water temperature: Paleoenvironmental implications of lake carbonate $\delta^{18}\text{O}$ and temperature records: *Earth and Planetary Science Letters*, v. 337–338, p. 77–84, <http://dx.doi.org/10.1016/j.epsl.2012.05.019>
- Hren, M. T., Pagani, M., Erwin, D. M., and Brandon, M., 2010, Biomarker reconstruction of the early Eocene paleotopography and paleoclimate of the northern Sierra Nevada: *Geology*, v. 38, n. 1, p. 7–10, <http://dx.doi.org/10.1130/G30215.1>
- Hurtado, J. M., Hodges, K. V., and Whipple, K. X., 2001, Neotectonics of the Thakkola graben and implications for recent activity on the South Tibetan fault system in the central Nepal Himalaya: *Geological Society of America Bulletin*, v. 113, n. 2, p. 222–240, [http://dx.doi.org/10.1130/0016-7606\(2001\)113<0222:NOTTGA>2.0.CO;2](http://dx.doi.org/10.1130/0016-7606(2001)113<0222:NOTTGA>2.0.CO;2)
- Huntington, K. W., Saylor, J., Quade, J., and Hudson, A. M., 2015, High late Miocene–Pliocene elevation of the Zhada Basin, southwestern Tibetan Plateau, from carbonate clumped isotope thermometry: *Geological Society of America Bulletin*, v. 127, n. 1–2, p. 181–199, <http://dx.doi.org/10.1130/B31000.1>
- Kelts, K., and Talbot, M. R., 1989, Lacustrine carbonates as geochemical archives of environmental change and biotic-abiotic interactions, *in* Tilzer, M. M., and Seruya, C., editors, *Ecological Structure and Function in Large Lakes: Madison, Wisconsin, Science and Technology Publishers*, p. 290–317.
- Khan, M. A., Spicer, R. A., Bera, S., Ghosh, R., Yang, J., Spicer, T. E. V., Guo, S. X., Su, T., Jacques, F., and Grote, P. J., 2014, Miocene to Pleistocene floras and climate of the Eastern Himalayan Siwaliks, and new palaeoelevation estimates for the Namling–Oiyug Basin, Tibet: *Global and Planetary Change*, v. 113, p. 1–10, <http://dx.doi.org/10.1016/j.gloplacha.2013.12.003>
- Kim, S. T., and O’Neil, J. R., 1997, Equilibrium and nonequilibrium oxygen isotope effects in synthetic carbonates: *Geochimica et Cosmochimica Acta*, v. 61, n. 16, p. 3461–3475, [http://dx.doi.org/10.1016/S0016-7037\(97\)00169-5](http://dx.doi.org/10.1016/S0016-7037(97)00169-5)
- Kim, S. T., Mucci, A., and Taylor, B. E., 2007, Phosphoric acid fractionation factors for calcite and aragonite between 25 and 75 °C: Revisited: *Chemical Geology*, v. 246, n. 3–4, p. 135–146, <http://dx.doi.org/10.1016/j.chemgeo.2007.08.005>
- LaRiviere, J. P., Ravelo, A. C., Crimmins, A., Dekens, P. S., Ford, H. L., Lyle, M., and Wara, M. W., 2012 Late Miocene decoupling of oceanic warmth and atmospheric carbon dioxide forcing: *Nature*, v. 486, p. 97–100, <http://dx.doi.org/10.1038/nature11200>
- Leier, A., Quade, J., DeCelles, P. G., and Kapp, P., 2009, Stable isotopic results from paleosol carbonate in south Asia: Paleoenvironmental reconstructions and selective alteration: *Earth and Planetary Science Letters*, v. 279, n. 3–4, p. 242–254, <http://dx.doi.org/10.1016/j.epsl.2008.12.044>
- Li, S., Currie, B. S., Rowley, D. B., and Ingalls, M., 2015, Cenozoic paleoaltimetry of the SE margin of the Tibetan Plateau: Constraints on the tectonic evolution of the region: *Earth and Planetary Science Letters*, v. 432, p. 415–424, <http://dx.doi.org/10.1016/j.epsl.2015.09.044>
- McInerney, F. A., Helliker, B. R., and Freeman, K. H., 2011, Hydrogen isotope ratios of leaf wax *n*-alkanes in grasses are insensitive to transpiration: *Geochimica et Cosmochimica Acta*, v. 75, n. 2, p. 541–554, <http://dx.doi.org/10.1016/j.gca.2010.10.022>
- McKenzie, J. A., 1982, Carbon-13 cycle in Lake Greifen: A model for restricted ocean basins, *in* Schlanger, S. O., and Cita, M. B., editors, *Nature and Origin of Cretaceous Carbon-Rich Facies*: New York, Academic Press, p. 197–207.
- Molnar, P., and Stock, J. M., 2009, Slowing of India’s convergence with Eurasia since 20 Ma and its implications for Tibetan mantle dynamic: *Tectonics*, v. 28, n. 3, TC3001, <http://dx.doi.org/10.1029/2008TC002271>
- Molnar, P., England, P., and Martinod, J., 1993, Mantle dynamics, uplift of the Tibetan Plateau, and the Indian Monsoon: *Reviews of Geophysics*, v. 31, n. 4, p. 357–396, <http://dx.doi.org/10.1029/93RG02030>
- Mora, C. I., Sheldon, B. T., Elliott, W. C., and Driese, S. G., 1998, An oxygen isotope study of illite and calcite in three Appalachian Paleozoic vertic paleosols: *Journal of Sedimentary Research*, v. 68, n. 3, p. 456–464, <http://dx.doi.org/10.2110/jsr.68.456>
- Mulch, A., Graham, S. A., and Chamberlain, C. P., 2006, Hydrogen isotopes in Eocene river gravels and paleoelevation of the Sierra Nevada: *Science*, v. 313, n. 5783, p. 87–89, <http://dx.doi.org/10.1126/science.1125986>
- Pedentchouk, N., Freeman, K. H., and Harris, N. B., 2006, Different response of δD values of *n*-alkanes, isoprenoids and kerogen during thermal maturation: *Geochimica et Cosmochimica Acta*, v. 70, n. 8, p. 2063–2072, <http://dx.doi.org/10.1016/j.gca.2006.01.013>
- Peters, K. E., Walters, C. C., and Moldovan, J. M., 2004, *The Biomarker Guide*, 2nd edition: Cambridge, United Kingdom, Cambridge University Press, 700 p.
- Philp, R. P., 1985, *Fossil fuel biomarkers: Applications and spectra*: New York, Elsevier Science Publishing Company, *Methods in Geochemistry and Geophysics*, v. 23, 298 p.
- Poage, M. A., and Chamberlain, C. P., 2001, Empirical relationships between elevation and the stable isotope composition of precipitation and surface waters: Considerations for studies of paleoelevation change: *American Journal of Science*, v. 301, n. 1, p. 1–15, <http://dx.doi.org/10.2475/ajs.301.1.1>

- Polissar, P. J., and D'Andrea, W. J., 2014, Uncertainty in Paleohydrologic reconstructions from molecular δD values: *Geochimica et Cosmochimica Acta*, v. 129, p. 146–156, <http://dx.doi.org/10.1016/j.gca.2013.12.021>
- Polissar, P. J., and Freeman, K. H., 2010, Effects of aridity and vegetation on plant-wax δD in modern lake sediments: *Geochimica et Cosmochimica Acta*, v. 74, n. 20, p. 5785–5797, <http://dx.doi.org/10.1016/j.gca.2010.06.018>
- Polissar, P. J., Freeman, K. H., Rowley, D. B., McInerney, F. A., and Currie, B. S., 2009, Paleoaltimetry of the Tibetan Plateau from D/H Ratios of Lipid Biomarkers: *Earth and Planetary Science Letters*, v. 287, n. 1–2, p. 64–76, <http://dx.doi.org/10.1016/j.epsl.2009.07.037>
- Quade, J., and Cerling, T. E., 1995, Expansion of C_4 grasses in the Late Miocene of Northern Pakistan: Evidence from stable isotopes in paleosols: *Palaeogeography, Palaeoclimatology, Palaeoecology*, v. 115, n. 1–4, p. 91–116, [http://dx.doi.org/10.1016/0031-0182\(94\)00108-K](http://dx.doi.org/10.1016/0031-0182(94)00108-K)
- Quade, J., Cerling, T. E., and Bowman, J. R., 1989, Development of Asian monsoon revealed by marked ecological shift during the latest Miocene in northern Pakistan: *Nature*, v. 342, p. 163–166, <http://dx.doi.org/10.1038/342163a0>
- Quade, J., Garzzone, C., and Eiler, J., 2007, Paleoelevation Reconstruction using Pedogenic Carbonates, *in* Kohn, M. J., editor, *Paleoaltimetry: Geochemical and Thermodynamic Approaches: Reviews in Mineralogy and Geochemistry*, v. 66, n. 1, p. 53–87, <http://dx.doi.org/10.2138/rmg.2007.66.3>
- Quade, J., Eiler, J., Daëron, M., and Achyuthan, H., 2013, The clumped isotope geothermometer in soil and paleosol carbonate: *Geochimica et Cosmochimica Acta*, v. 105, p. 92–107, <http://dx.doi.org/10.1016/j.gca.2012.11.031>
- Rezaee, M. R., Lemon, N. M., and Seggie, R. J., 1997, Tectonic fingerprints in siderite cement, Tirrawarra Sandstone, southern Cooper Basin, Australia: *Geological Magazine*, v. 134, n. 1, p. 99–112, <http://dx.doi.org/10.1017/S0016756897006407>
- Rosen, M. R., Turner, J. V., Coshell, L., and Gailitis, V., 1995, The effects of water temperature, stratification, and biological activity on the stable isotopic composition and timing of carbonate precipitation in a hypersaline lake: *Geochimica et Cosmochimica Acta*, v. 59, n. 5, p. 979–990, [http://dx.doi.org/10.1016/0016-7037\(95\)00016-X](http://dx.doi.org/10.1016/0016-7037(95)00016-X)
- Rosenbaum, J., and Sheppard, S. M. F., 1986, An isotopic study of siderites, dolomites and ankerites at high temperatures: *Geochimica et Cosmochimica Acta*, v. 50, n. 6, p. 1147–1150, [http://dx.doi.org/10.1016/0016-7037\(86\)90396-0](http://dx.doi.org/10.1016/0016-7037(86)90396-0)
- Rowley, D. B., 2007, Stable Isotope-Based Paleoaltimetry: Theory and Validation, *in* Kohn, M. J., editor, *Paleoaltimetry: Geochemical and Thermodynamic Approaches: Reviews in Mineralogy and Geochemistry*, v. 66, n. 1, p. 23–52, <http://dx.doi.org/10.2138/rmg.2007.66.2>
- Rowley, D. B., and Currie, B. S., 2006, Palaeo-altimetry of the late Eocene to Miocene Lunpola basin, central Tibet: *Nature*, v. 439, p. 677–681, <http://dx.doi.org/10.1038/nature04506>
- Rowley, D. B., and Garzzone, C. E., 2007, Stable isotope-based paleoaltimetry: *Annual Review of Earth and Planetary Sciences*, v. 35, p. 463–508, <http://dx.doi.org/10.1146/annurev.earth.35.031306.140155>
- Rowley, D. B., Pierrehumbert, R. T., and Currie, B. S., 2001, A new approach to stable isotope-based paleoaltimetry: Implications for paleoaltimetry and paleohypsometry of the high Himalaya since the late Miocene: *Earth and Planetary Science Letters*, v. 188, n. 1–2, p. 253–268, [http://dx.doi.org/10.1016/S0012-821X\(01\)00324-7](http://dx.doi.org/10.1016/S0012-821X(01)00324-7)
- Rozanski, K., Araguás-Araguás, L., and Gonfiantini, R., 1993, Isotopic Patterns in Modern Global Precipitation, *in* Swart, P. K., Lohmann, K. C., McKenzie, J., and Savin, S., editors, *Climate Change in Continental Isotopic Records: American Geophysical Union Geophysical Monograph Series 78*, p. 1–36, <http://dx.doi.org/10.1029/GM078p0001>
- Sachse, D., Billault, I., Bowen, G. J., Chikaraishi, Y., Dawson, T. E., Feakins, S. J., Freeman, K. H., Magill, C. R., McInerney, F. A., van der Meer, M. T. J., Polissar, P., Robins, R. J., Sachs, J. P., Schmidt, H. L., Sessions, A. L., White, J. W. C., West, J. B., and Kahmen, A., 2012, Molecular Paleohydrology: Interpreting the Hydrogen-Isotopic Composition of Lipid Biomarkers from Photosynthesizing Organisms: *Annual Review of Earth and Planetary Sciences*, v. 40, p. 221–249, <http://dx.doi.org/10.1146/annurev-earth-042711-105535>
- Saylor, J. E., Quade, J., Dettman, D. L., DeCelles, P. G., Kapp, P. A., and Ding, L., 2009, The late Miocene through present paleoelevation history of southwestern Tibet: *American Journal of Science*, v. 309, n. 1, p. 1–42, <http://dx.doi.org/10.2475/01.2009.01>
- Saylor, J., DeCelles, P., Gehrels, G., Murphy, M., Zhang, R., and Kapp, P., 2010, Basin formation in the High Himalaya by arc-parallel extension and tectonic damming: Zhada basin, southwestern Tibet: *Tectonics*, v. 29, n. 1, TC1004, <http://dx.doi.org/10.1029/2008TC002390>
- Schimmelmann, A., Sessions, A. L., and Mastalerz, M., 2006, Hydrogen isotopic (D/H) composition of organic matter during diagenesis and thermal maturation: *Annual Review of Earth and Planetary Sciences*, v. 34, p. 501–533, <http://dx.doi.org/10.1146/annurev.earth.34.031405.125011>
- Sessions, A. L., Burgoyne, T. W., and Hayes, J. M., 2001, Correction of H_3^+ Contributions in Hydrogen Isotope Ratio Monitoring Mass Spectrometry: *Analytical Chemistry*, v. 73, n. 2, p. 192–199, <http://dx.doi.org/10.1021/ac000489e>
- Spicer, R. A., Harris, N. B. W., Widdowson, M., Herman, A. B., Guo, S., Valdes, P. J., Wolfe, J. A., and Kelley, S. P., 2003, Constant elevation of southern Tibet over the past 15 million years: *Nature*, v. 421, p. 622–624, <http://dx.doi.org/10.1038/nature01356>
- Stewart, D. R. M., Pearson, P. N., Ditchfield, P. W., and Singano, J. M., 2004, Miocene tropical Indian Ocean temperatures: Evidence from three exceptionally preserved foraminiferal assemblages in Tanzania: *Journal of African Earth Sciences*, v. 40, n. 3–4, p. 173–190, <http://dx.doi.org/10.1016/j.jafrearsci.2004.09.001>
- Talbot, M. R., 1990, A review of the paleohydrological interpretation of carbon and oxygen isotopic ratios in

- primary lacustrine carbonates: *Chemical Geology*, v. 80, n. 4, p. 261–279, [http://dx.doi.org/10.1016/0168-9622\(90\)90009-2](http://dx.doi.org/10.1016/0168-9622(90)90009-2)
- Thompson, L. G., Yao, T., Mosley-Thompson, E., Davis, M. E., Henderson, K. A., and Lin, P.-N., 2000, A High-Resolution Millennial Record of the South Asian Monsoon from Himalayan Ice Cores: *Science*, v. 289, n. 5486, p. 1916–1919, <http://dx.doi.org/10.1126/science.289.5486.1916>
- Teranes, J. L., McKenzie, J. A., Bernasconi, S. M., Lotter, A. F., and Sturm, M., 1999, A study of oxygen isotopic fractionation during bio-induced calcite precipitation in eutrophic Baldeggersee, Switzerland: *Geochimica et Cosmochimica Acta*, v. 63, n. 13–14, p. 1981–1989, [http://dx.doi.org/10.1016/S0016-7037\(99\)00049-6](http://dx.doi.org/10.1016/S0016-7037(99)00049-6)
- Vasconcelos, C., McKenzie, J. A., Warthmann, R., and Bernasconi, S. M., 2005, Calibration of the delta O-18 paleothermometer for dolomite precipitated in microbial cultures and natural environments: *Geology*, v. 33, n. 4, p. 317–320, <http://dx.doi.org/10.1130/G20992.1>
- Wang, J., and Chen, Y., 1999, Sedimentary formation characteristics of hydrocarbon generation and oil exploration prospects of Wuyu basin in Tibet: *Petroleum Exploration and Development*, v. 26, n. 4, p. 14–17.
- Zhang, C. L., Horita, J., Cole, D. R., Zhou, J. Z., Lovley, D. R., and Phelps, T. J., 2001, Temperature-dependent oxygen and carbon isotope fractionations of biogenic siderite: *Geochimica et Cosmochimica Acta*, v. 65, n. 14, p. 2257–2271, [http://dx.doi.org/10.1016/S0016-7037\(01\)00596-8](http://dx.doi.org/10.1016/S0016-7037(01)00596-8)
- Zhang, Y. G., Pagani, M., Liu, Z., Bohaty, S. M., and DeConto, R., 2013, A 40 million year history of atmospheric CO₂: *Philosophical Transactions of the Royal Society A*, v. 371, n. 2001, <http://dx.doi.org/10.1098/rsta.2013.0096>
- Zhang, Y. G., Pagani, M., and Liu, Z., 2014, A 12-Million-Year Temperature History of the Tropical Pacific Ocean: *Science*, v. 344, n. 6179, p. 84–87, <http://dx.doi.org/10.1126/science.1246172>
- Zhou, S., Mo, X. X., Zhao, Z. D., Qiu, R. Z., Niu, Y. L., Guo, T. Y., and Zhang, S. Q., 2010a, ⁴⁰Ar/³⁹Ar Geochronology of post-collisional volcanism in the middle Gangdese Belt, southern Tibet: *Journal of Asian Earth Sciences*, v. 37, n. 3, p. 246–258, <http://dx.doi.org/10.1016/j.jseas.2009.08.011>
- Zhou, Y., Grice, K., Stuart-Williams, H., Farquhar, G. D., Hocart, C. H., Lu, H., and Liu, W., 2010b, Biosynthetic origin of the saw-toothed profile in δ¹³C and δ²H of *n*-alkanes and systematic isotopic differences between *n*-, *iso*- and *anteiso*-alkanes in leaf waxes of land plants: *Phytochemistry*, v. 71, n. 4, p. 388–403, <http://dx.doi.org/10.1016/j.phytochem.2009.11.009>
- Zhu, Y., Fang, X., Gao, J., Yi, H., Wang, S., and Zhang, W., 2006, Oligo-Miocene depositional facies of the Wuyu basin, southern Tibetan Plateau: *Acta Sedimentologica Sinica*, v. 24, p. 775–782.